became apparent at 48 hours or later; 1.2-, 2.2-, and 5.1-fold higher than that in controls at 24, 48, and 72 hours after administration, respectively (Fig. 3C), and this effect was dose dependent ($p < 0.001$, Jonckheere–Terpstra test; Fig. 3D).

The effect of HMW-/MMW-adiponectin on the expression of TIMP-1 in fibroblasts was similar to that on the expression of MMP-1 and MMP-3, with an apparent dose-dependent effect at 48 hours or later (Fig. 3E and F). In contrast, the effect of HMW-/MMW-adiponectin on the expression of TIMP-3 appeared earlier: 1.8-, 3.1-, and 2.3-fold higher than that in controls at 24, 48, and 72 hours after administration, respectively, although the total expression started to decrease 48 hours after administration in wells with and without adiponectin (Fig. 3G). The effect of HMW-/MMW-adiponectin on the expression of TIMP-3 was also dose dependent ($p < 0.001$, Jonckheere–Terpstra test; Fig. 3H).

Immunofluorescent microscopy

Based on our observations, we assessed whether HMW-/MMW-adiponectin could produce or degrade ECMs in vitro. Under the current experimental setting, HMW-/MMW-adiponectin seemed to induce greater synthesis and deposition of both fibronectin and collagen type 1 than that in the control, and the effect seemed to be comparable to that of TGF-β1 (Fig. 4).

TGF-β1 and TGF-βR2 expression

Next, we assessed whether HMW-/MMW-adiponectin would produce TGF-β1 and TGF-βR2, a well-known fibrogenic cytokine and receptor. There was no significant difference in the expression of TGF-β1 between fibroblasts with and without HMW-/MMW-adiponectin in this experimental setting (Fig. 5A and B). On the other hand, the expression of TGF-βR2 was 1.9- and 1.6-fold higher than that in the control group at 48 and 72 hours after administration, respectively (Fig. 5C). The expression of TGF-βR2 was dose-dependently higher than that in the control group; 1.6-, 1.8-, 2.2-, and 3.4-fold in wells with 1, 5, 10, and 20 μg/mL of HMW-/MMW-adiponectin, respectively ($p < 0.001$, Jonckheere–Terpstra test; Fig. 5D).

Effect of HMW-/MMW-adiponectin under TGF-βR2–blocked conditions

Next, we assessed whether the effect of HMW-/MMW-adiponectin was dependent on a TGF-β pathway under TGF-βR2–blocked conditions. The increased expression of ECMs, MMPs, and TIMPs by HMW-/MMW-adiponectin was not suppressed by the addition of anti–TGF-βR2 antibody (Fig. 6A–F).

Immunohistochemistry analysis of skin cGVHD

Immunohistochemistry was performed for samples of a normal subject, cGVHD-involved and noninvolved skin region of a patient with skin cGVHD. A diffuse increase of fibronectin expression with strong staining was observed in dermis of the involved region of skin cGVHD compared with normal skin and noninvolved region of skin cGVHD (Fig. 7). TGF-βR2, MMP-3, and MCP-1 were stained mainly in ducts and endothelial cells. An increase of spindle cells that express TGF-βR2 (strong staining), MMP-3 (relatively weak staining), and MCP-1 (weak and small amount) were observed especially in papillary dermis of the involved region of skin cGVHD compared with normal skin and noninvolved region of skin cGVHD (Fig. 7). In addition, they were increased in epidermis of both involved and noninvolved skin regions of the patient compared with normal skin. Cells with MMP-1 expression were also observed in the dermis of the involved region of skin cGVHD, although they were few in number and sporadic with a weak staining (Fig. 7). On the other hand, we could not find any differences in the expressions of TIMP-1 and TIMP-3.

Discussion

Adiponectin has been shown to have both proinflammatory and anti-inflammatory functions [12]. In obesity-related diseases such as diabetes mellitus, adiponectin is thought to induce IL-10, and to have anti-inflammatory effects and protect against cardiovascular events [10,11]. On the other hand, high adiponectin levels have been observed and associated with the disease severity in autoimmune diseases including rheumatoid arthritis, systemic lupus erythematosus, inflammatory bowel disease, and diabetes mellitus type 1 [15,17,28–31]. In addition, adiponectin stimulated the secretion of proinflammatory cytokines, including IL-6, IL-8, and MMPs, in animal models [32]. Although there have been few reports on systemic sclerosis, high adiponectin levels were positively correlated to disease duration and a high skin-thickness score [33]. In addition, it has been shown that the skin of nonobese people, who are thought to have higher adiponectin levels, is thicker than that of obese people [34].

The controversy regarding whether adiponectin has a proinflammatory or anti- inflammatory effect might be due to the fact that most observations and animal models have been based on the use of mixtures of all of the isoforms of adiponectin. Recently, it has been suggested that adiponectin might have different effects on different target cells and tissues, and that its functions might be different according to its isoforms [16,17]. Therefore, we used only HMW-/MMW-adiponectin in our experiments. In addition, no previous study has assessed the effect of adiponectin on not only ECM but also both MMPs and TIMPs in human dermal fibroblasts (Table 1) [35–42]. Therefore, we assessed the effects of HMW-/MMW-adiponectin on human dermal fibroblasts.

The current study showed that HMW-/MMW-adiponectin induced higher gene expression and synthesis of FN1 in dermal fibroblasts. On the other hand, HMW-/MMW-adiponectin did not affect the gene expression of COL1A2, but

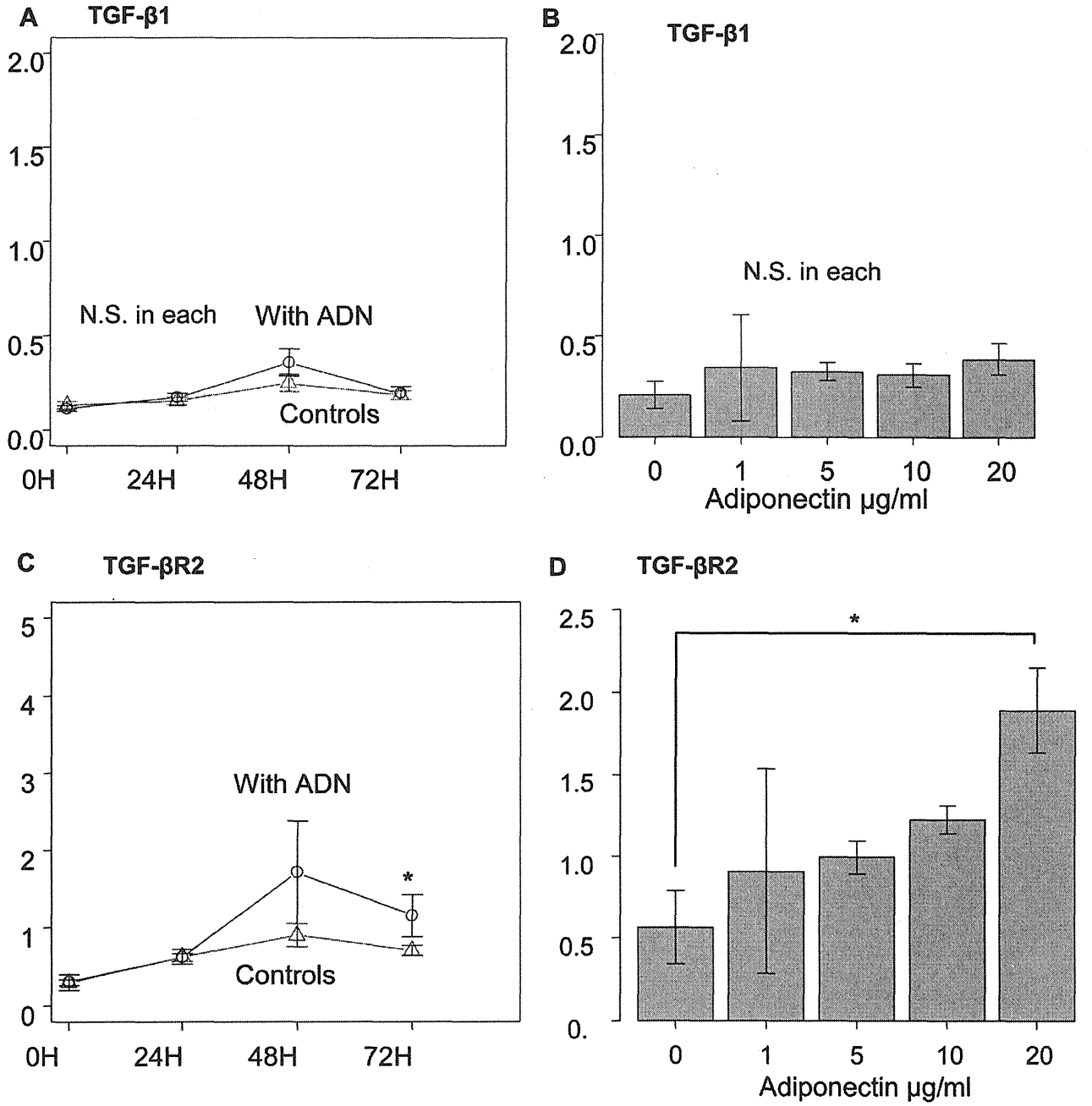

Figure 5. Comparisons of the relative transcripts of TGF-β1 and TGF-βR2. Comparisons of the expression of TGF-β1 **(A, B)** and TGF-βR2 **(C, D)** evaluated with qRT-PCR—**(A, C)** in a time-dependent manner at 0, 24, 48, and 72 hours after 0 or 10 μg/mL of high- or middle-molecular-weight-adiponectin administration and **(B, D)** in a dose-dependent manner 3 days after adiponectin administration (0, 1, 5, 10, or 20 μg/mL). The comparisons are shown between target and control cells. $*p < 0.05$; $**p < 0.01$; $***p < 0.005$.

did induce the greater deposition of collagen type 1 than in the control, which is consistent with a previous report that adiponectin upregulates the secretions but not the gene expression of collagen [43].

It is well known that TGF-β1 is associated with the accumulation of ECMs and fibrosis [19,20]. HMW-/MMW-adiponectin did not have a significant effect on the expression of TGF-β1. On the other hand, it significantly upregulated the expression of TGF-βR2. However, the promoting effects of HMW-/MMW-adiponectin on ECM expression were not suppressed by the neutralization of TGF-βR2. Therefore, HWM-/MMW-adiponectin can increase the expression of ECM independent from the TGF-βR2 pathways.

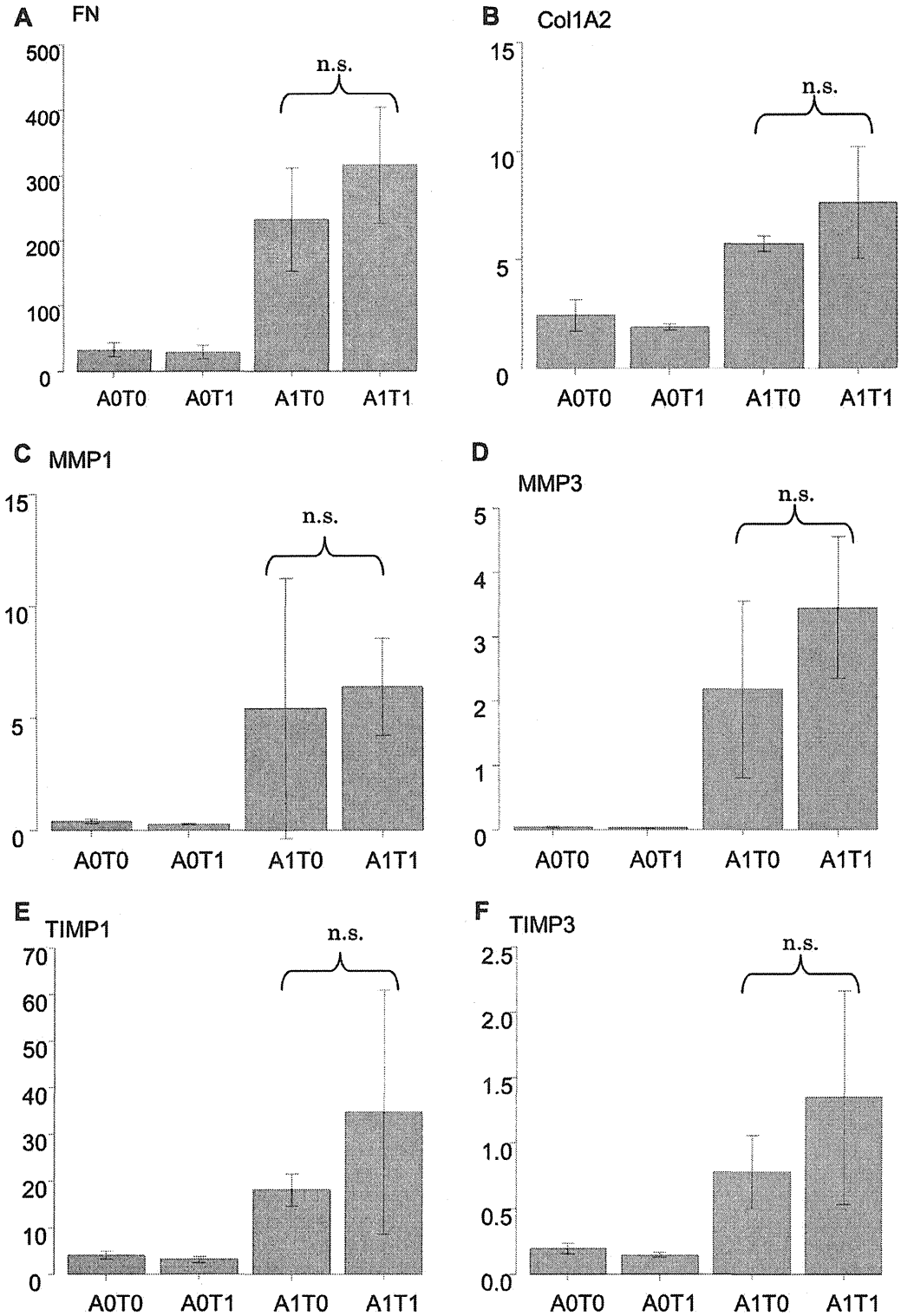

Figure 6. Comparisons of the relative transcripts of extracellular matrix and metalloproteinase families with or without blocking of the TGF-βR2 pathway. The expression of **(A)** fibronectin 1 (FN1), **(B)** collagen type1 α 2 (COL1A2), **(C)** MMP-1, **(D)** MMP-3, **(E)** TIMP-1, and **(F)** TIMP-3 were evaluated with qRT-PCR and compared in cells without both adiponectin and anti–TGF-βR2 antibody (A0T0), without adiponectin but with 20 μg/mL of anti–TGF-βR2 antibody (A0T1), with 20 μg/mL of adiponectin but without anti–TGF-βR2 antibody (A1T0), and with 20 μg/mL of both adiponectin and anti–TGF-βR2 antibody (A1T1) at 3 days after administration.

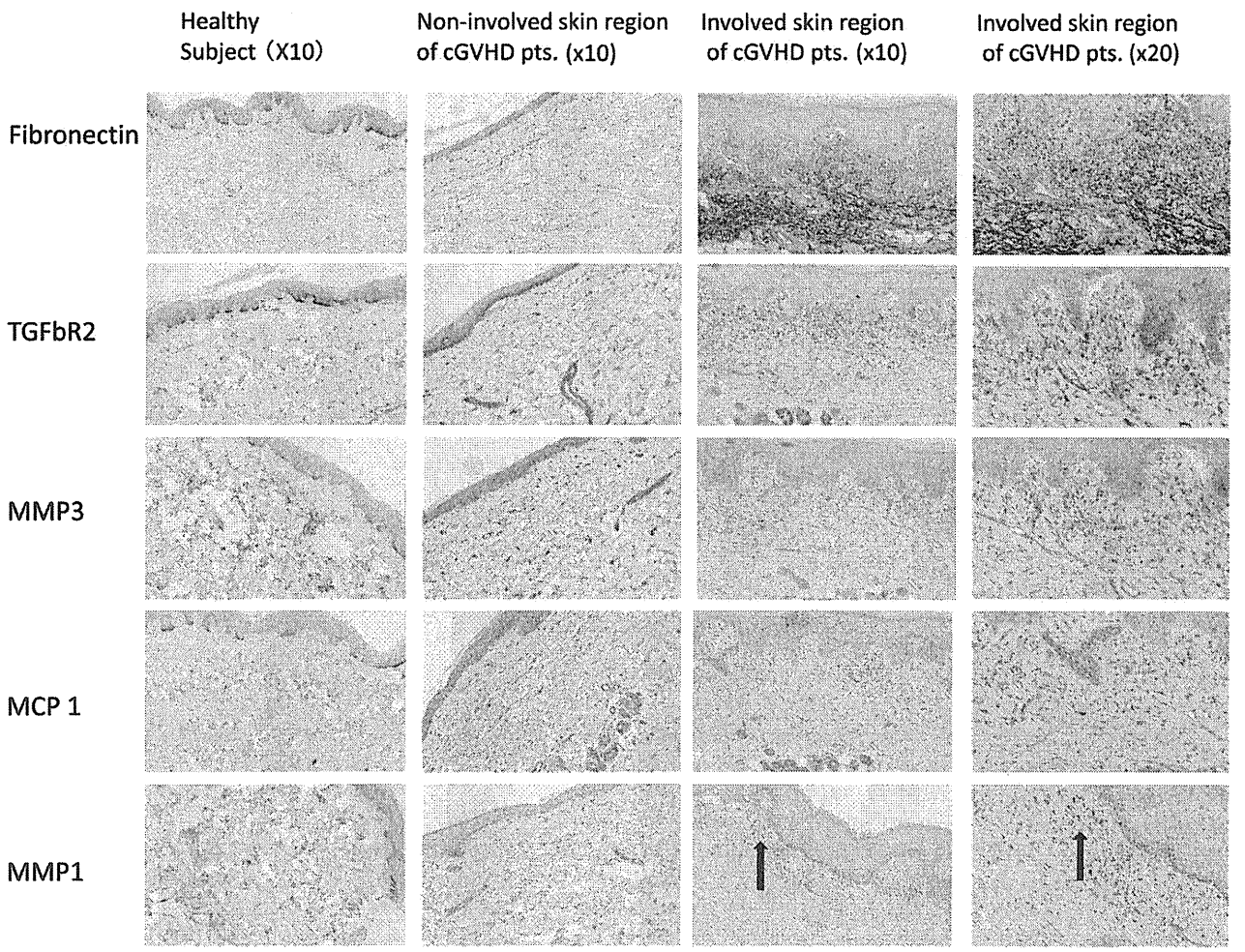

Figure 7. Immunohistochemistry was performed using formalin-fixed paraffin-embedded skin samples of a healthy subject and a patient with skin cGVHD for fibronectin, TGF-βR2, MMP-3, MCP-1, and MMP-1. EnVision immunohistochemistry stain. The blue arrows indicate positive regions for MMP-1.

Table 1. Summary of other investigations that have assessed the effects of adiponectin on both MMPs and TIMPs[a]

Adiponectin isoform	Target cell	Matrix metalloproteinase (MMP)	Tissue inhibitor of metalloproteinase (TIMP)	Reference
Full-length adiponectin, trimers	—	MMP-9 gene expression ↑	TIMP-1 expression ↑	[35]
In vivo study using knockout vs. wild type mice	Rat and mouse cardiomyocyte	ROS-induced MMP-2 and MMP-9 activity ↓	MMP-2-to-TIMP-2 and MMP-9-to-TIMP-1 ratios ↑ in knockout mice	[36]
Full-length adiponectin, trimers	Human chondrocytes of osteoarthritis	MMP-1, MMP-3, and MMP-13 expression and secretion ↑	TIMP-1 expression, no change	[37]
No details	Human trophoblast	MMP-2 and MMP-9 activity ↑	TIMP-1 expression, no change TIMP-2 expression ↓	[38]
No details	Rat hepatic stellate cells	MMP-1 activity ↑	Leptin-stimulated TIMP-1 ↓	[39]
Full-length adiponectin, Trimers	Human and murine chondrocytes	MMP-3 and MMP-9 secretion ↑ MMP-2 secretion, no change	TIMP-1 secretion, no change	[40]
Full-length adiponectin, trimers	Human chondrocyte	IL-β–induced MMP-13 expression ↑ MMP-3 expression, no change	TIMP-2 expression ↑ TIMP-1 expression, no change	[41]
No details	Human monocyte -derived macrophages	MMP-9 expression, no change	TIMP-1 expression ↑	[42]

[a]Data from http://www.ncbi.nlm.nih.gov/pubmed/, using the search terms *adiponectin*, *MMP*, and *TIMP*.

HMW-/MMW-adiponectin not only induced the synthesis and deposition of ECMs; it also upregulated the expression of both TIMPs and MMPs. These findings are consistent with the observation that TIMP-1, MMP-1, and MMP-3 are all increased in dermal fibroblasts in the early stages of systemic sclerosis, whereas MMP-1 and MMP-3 are decreased in the late stages [26]. Taken together, these findings suggest that HMW-/MMW-adiponectin can modulate dermal fibrotic pathways. However, the current findings were obtained in vitro, and thus do not directly show fibrosis in vivo by HMW-/MMW-adiponectin. In fact, the IHC of skin cGVHD actually showed certain increases in the expressions of fibronectin, TGF-βR2, and MMP-3, but not of TIMPs. These IHC findings suggest that cGVHD could not be explained only by adiponectin, although skin biopsy samples from only one patient were too small to establish a definite conclusion. The association between adiponectin and skin cGVHD scores should be evaluated in future prospective trials.

Other possible limitations of our study are that the assessment time of the current fibroblast analysis was different from the actual development of skin cGVHD and that not only long-term steroid administration but also autopsy samples might affect our IHC results.

The symptoms of cGVHD are diverse and complicated, beyond just simple skin fibrosis. Therefore, the role of HMW-adiponectin in the network of cGVHD in vivo remains to be elucidated. Further basic investigations are needed to clarify how HMW-/MMW-adiponectin can play a role in ECM regulation and the pathophysiology of sclerotic cGVHD in vivo, and whether the adiponectin-pathway could be a target for the treatment of sclerotic cGVHD.

Acknowledgments

This study was partially supported by The Research Award to Jichi Medical University Graduate Student (H.N.).

Author contributions: H.N. designed the study, performed experiments, analyzed data, and wrote the manuscript; K.T-S., R. Yamazaki, M.S, Y.T., K.S., M.K., R. Yamasaki, H.W., Y.I, K.K, T.M, M.A., S. Kimura, M.K., S.O., A.T., J.K., S. Kako, and J.N. collected data and gave their advice about the experimental procedures; Y.S. collected and analyzed pathologic findings; Y.K. designed the study, analyzed data, and wrote the manuscript.

Conflict of interest disclosure

No financial interest/relationships with financial interest relating to the topic of this article have been declared.

References

1. Paczesny S, Hanauer D, Sun Y, Reddy P. New perspectives on the biology of acute GVHD. Bone Marrow Transplant. 2010;45:1–11.
2. Sarantopoulos S, Stevenson KE, Kim HT, et al. Altered B-cell homeostasis and excess BAFF in human chronic graft-versus-host disease. Blood. 2009;113:3865–3874.
3. Shimabukuro-Vornhagen A, Hallek MJ, Storb RF, von Bergwelt-Baildon MS. The role of B cells in the pathogenesis of graft-versus-host disease. Blood. 2009;114:4919–4927.
4. Ferrara JL, Levine JE, Reddy P, Holler E. Graft-versus-host disease. Lancet. 2009;373:1550–1561.
5. Pidala J, Anasetti C, Jim H. Quality of life after allogeneic hematopoietic cell transplantation. Blood. 2009;114:7–19.
6. Schultz KR, Miklos DB, Fowler D, et al. Toward biomarkers for chronic graft-versus-host disease: National Institutes of Health consensus development project on criteria for clinical trials in chronic graft-versus-host disease: III. Biomarker Working Group Report. Biol Blood Marrow Transplant. 2006;12:126–137.
7. Fujii H, Cuvelier G, She K, et al. Biomarkers in newly diagnosed pediatric-extensive chronic graft-versus-host disease: a report from the Children's Oncology Group. Blood. 2008;111:3276–3285.
8. Imamura M, Hashino S, Kobayashi H, et al. Serum cytokine levels in bone marrow transplantation: synergistic interaction of interleukin-6, interferon-gamma, and tumor necrosis factor-alpha in graft-versus-host disease. Bone Marrow Transplant. 1994;13:745–751.
9. Liem LM, van Houwelingen HC, Goulmy E. Serum cytokine levels after HLA-identical bone marrow transplantation. Transplantation. 1998;66:863–871.
10. Yamauchi T, Kadowaki T. Physiological and pathophysiological roles of adiponectin and adiponectin receptors in the integrated regulation of metabolic and cardiovascular diseases. Int J Obes (Lond). 2008; 32(Suppl 7):S13–S18.
11. Stofkova A. Leptin and adiponectin: from energy and metabolic dysbalance to inflammation and autoimmunity. Endocr Regul. 2009;43:157–168.
12. Fantuzzi G. Adiponectin and inflammation: consensus and controversy. J Allergy Clin Immunol. 2008;121:326–330.
13. Tilg H, Moschen AR. Role of adiponectin and PBEF/visfatin as regulators of inflammation: involvement in obesity-associated diseases. Clin Sci (Lond). 2008;114:275–288.
14. Otero M, Lago R, Gomez R, et al. Changes in plasma levels of fat-derived hormones adiponectin, leptin, resistin and visfatin in patients with rheumatoid arthritis. Ann Rheum Dis. 2006;65:1198–1201.
15. Yamamoto K, Kiyohara T, Murayama Y, et al. Production of adiponectin, an anti-inflammatory protein, in mesenteric adipose tissue in Crohn's disease. Gut. 2005;54:789–796.
16. Brochu-Gaudreau K, Rehfeldt C, Blouin R, Bordignon V, Murphy BD, Palin MF. Adiponectin action from head to toe. Endocrine. 2010;37: 11–32.
17. Neumann E, Frommer KW, Vasile M, Muller-Ladner U. Adipocytokines as driving forces in rheumatoid arthritis and related inflammatory diseases? Arthritis Rheum. 2011;63:1159–1169.
18. Nakasone H, Binh PN, Yamazaki R, et al. Association between serum high-molecular-weight adiponectin level and the severity of chronic graft-versus-host disease in allogeneic stem cell transplantation recipients. Blood. 2011;117:3469–3472.
19. Jinnin M. Mechanisms of skin fibrosis in systemic sclerosis. J Dermatol. 2010;37:11–25.
20. Cotton SA, Herrick AL, Jayson MI, Freemont AJ. TGF beta–a role in systemic sclerosis? J Pathol. 1998;184:4–6.
21. Tsang ML, Zhou L, Zheng BL, et al. Characterization of recombinant soluble human transforming growth factor-beta receptor type II (rhTGF-beta sRII). Cytokine. 1995;7:389–397.
22. Lareu RR, Subramhanya KH, Peng Y, et al. Collagen matrix deposition is dramatically enhanced in vitro when crowded with charged macromolecules: the biological relevance of the excluded volume effect. FEBS Lett. 2007;581:2709–2714.
23. Chen CZ, Peng YX, Wang ZB, et al. The Scar-in-a-Jar: studying potential antifibrotic compounds from the epigenetic to extracellular level in a single well. Br J Pharmacol. 2009;158:1196–1209.

24. Karamichos D, Guo XQ, Hutcheon AE, Zieske JD. Human corneal fibrosis: an in vitro model. Invest Ophthalmol Vis Sci. 2010;51: 1382–1388.
25. Ivanov D, Philippova M, Antropova J, et al. Expression of cell adhesion molecule T-cadherin in the human vasculature. Histochem Cell Biol. 2001;115:231–242.
26. Kuroda K, Shinkai H. Gene expression of types I and III collagen, decorin, matrix metalloproteinases and tissue inhibitors of metalloproteinases in skin fibroblasts from patients with systemic sclerosis. Arch Dermatol Res. 1997;289:567–572.
27. Salmela MT, Karjalainen-Lindsberg ML, Jeskanen L, Saarialho-Kere U. Overexpression of tissue inhibitor of metalloproteinases-3 in intestinal and cutaneous lesions of graft-versus-host disease. Mod Pathol. 2003;16:108–114.
28. Ebina K, Fukuhara A, Ando W, et al. Serum adiponectin concentrations correlate with severity of rheumatoid arthritis evaluated by extent of joint destruction. Clin Rheumatol. 2009;28:445–451.
29. Hadjadj S, Aubert R, Fumeron F, et al. Increased plasma adiponectin concentrations are associated with microangiopathy in type 1 diabetic subjects. Diabetologia. 2005;48:1088–1092.
30. Rovin BH, Song H, Hebert LA, et al. Plasma, urine, and renal expression of adiponectin in human systemic lupus erythematosus. Kidney Int. 2005;68:1825–1833.
31. Fayad R, Pini M, Sennello JA, et al. Adiponectin deficiency protects mice from chemically induced colonic inflammation. Gastroenterology. 2007;132:601–614.
32. Ehling A, Schaffler A, Herfarth H, et al. The potential of adiponectin in driving arthritis. J Immunol. 2006;176:4468–4478.
33. Masui Y, Asano Y, Shibata S, et al. Serum adiponectin levels inversely correlate with the activity of progressive skin sclerosis in patients with diffuse cutaneous systemic sclerosis. J Eur Acad Dermatol Venereol. 2011;26:354–360.
34. Smalls LK, Randall Wickett R, Visscher MO. Effect of dermal thickness, tissue composition, and body site on skin biomechanical properties. Skin Res Technol. 2006;12:43–49.
35. Wanninger J, Walter R, Bauer S, et al. MMP-9 activity is increased by adiponectin in primary human hepatocytes but even negatively correlates with serum adiponectin in a rodent model of non-alcoholic steatohepatitis. Exp Mol Pathol. 2011;91:603–607.
36. Essick EE, Ouchi N, Wilson RM, et al. Adiponectin mediates cardioprotection in oxidative stress-induced cardiac myocyte remodeling. Am J Physiol Heart Circ Physiol. 2011;301:H984–H993.
37. Kang EH, Lee YJ, Kim TK, et al. Adiponectin is a potential catabolic mediator in osteoarthritis cartilage. Arthritis Res Ther. 2010; 12:R231.
38. Benaitreau D, Dos Santos E, Leneveu MC, et al. Effects of adiponectin on human trophoblast invasion. J Endocrinol. 2010;207:45–53.
39. Handy JA, Saxena NK, Fu P, et al. Adiponectin activation of AMPK disrupts leptin-mediated hepatic fibrosis via suppressors of cytokine signaling (SOCS-3). J Cell Biochem. 2010;110:1195–1207.
40. Lago R, Gomez R, Otero M, et al. A new player in cartilage homeostasis: adiponectin induces nitric oxide synthase type II and pro-inflammatory cytokines in chondrocytes. Osteoarthritis Cartilage. 2008;16:1101–1109.
41. Chen TH, Chen L, Hsieh MS, Chang CP, Chou DT, Tsai SH. Evidence for a protective role for adiponectin in osteoarthritis. Biochim Biophys Acta. 2006;1762:711–718.
42. Kumada M, Kihara S, Ouchi N, et al. Adiponectin specifically increased tissue inhibitor of metalloproteinase-1 through interleukin-10 expression in human macrophages. Circulation. 2004;109:2046–2049.
43. Ezure T, Amano S. Adiponectin and leptin up-regulate extracellular matrix production by dermal fibroblasts. Biofactors. 2007;31:229–236.
44. Kanda Y. Investigation of the freely available easy-to-use software 'EZR' for medical statistics. Bone Marrow Transplant. 2013;48: 452–458.

Bone Marrow Transplantation (2014) **49**, 87–94

www.nature.com/bmt

ORIGINAL ARTICLE

Single-cell T-cell receptor-β analysis of HLA-A*2402-restricted CMV- pp65-specific cytotoxic T-cells in allogeneic hematopoietic SCT

H Nakasone, Y Tanaka, R Yamazaki, K Terasako, M Sato, K Sakamoto, R Yamasaki, H Wada, Y Ishihara, K Kawamura, T Machishima, M Ashizawa, S-i Kimura, M Kikuchi, A Tanihara, J Kanda, S Kako, J Nishida and Y Kanda

Cellular immunity is important for the control of CMV infection after allogeneic hematopoietic cell transplantation (Allo-HCT). However, the actual *in vivo* dynamics of CMV-specific cytotoxic T cell (CMV-CTL) clones are still unclear. We conducted clone monitoring of tetramer$^+$ CMV-CTLs in HLA-A*2402-positive donor–patient pairs, using a direct single-cell analysis that enabled the simultaneous identification and quantification of CTL clones. Clone dynamics were assessed in three cases with or without CMV reactivation. In Case-1 without CMV reactivation, despite the long-term use of systemic steroid, dominant clones of Donor-1 persisted and remained dominant. The CMV-CTLs at 1 year after Allo-HCT included a high proportion of CD45RA$^+$CCR7$^-$ effector and CD27$^-$CD57$^+$ mature T cells. On the other hand, in Cases-2 and -3 with CMV reactivation, novel clones appeared and became dominant during the follow-up. Their CMV-CTLs included more CD27$^+$ immature T cells at 1 year after Allo-HCT. With regard to clonotypes, HLA-A*2402-restricted CMV-CTLs tended to select BV7 and BJ1-1 genes for complementarity-determining region 3 (CDR3) of T-cell receptor (TCR)-β. Specific amino-acid sequences of CDR3 of TCR-β were found in each case. Patterns of clone reconstitution and phenotype would be different according to CMV reactivation. *In vivo* clone monitoring of CMV-CTLs could provide insight into the mechanism of immunological reconstitution following Allo-HCT.

Bone Marrow Transplantation (2014) **49**, 87–94; doi:10.1038/bmt.2013.122; published online 12 August 2013

Keywords: HLA-A*2402-restricted CMV-specific cytotoxic T cells; T-cell receptor-β; single-cell analysis; clone monitoring

INTRODUCTION

CMV reactivation is one of the major concerns after allogeneic hematopoietic cell transplantation (Allo-HCT).[1,2] It is important to control CMV reactivation before it progresses to diseases such as pneumonia because CMV diseases are associated with high mortality.[3,4] In addition to recent pre-emptive therapy, immunological reconstitution against CMV is necessary for long-term suppression of CMV reactivation.

Cellular immunity by CMV-specific cytotoxic T cells (CMV-CTL) is considered to have a major role in the control of CMV reactivation after Allo-HCT. HLA-restricted CMV-CTLs are identified by tetramer methods.[5,6] An individual CTL has a specific complementarity-determining region 3 (CDR3) of the T-cell receptor (TCR)-β, which is a result of the recombination of somatic TCR V-(D)-J genes and junction diversity. The repertoire of TCR and clones of CMV-CTLs have thus far been identified after *in vitro* bulk expansion, and therefore the results obtained to date may have been affected by the potential proliferation of CMV-CTL clones and bacterial-transforming efficiency.[7–10] Recently, we and others have developed a direct single-cell RT-PCR analysis that enables the simultaneous identification and quantification of CTL clones without the effects of *in vitro* expansion.[11,12] To the best of our knowledge, the *in vivo* dynamics and monitoring of CMV-CTL clones have not been assessed in Allo-HCT. In addition, the clonotypes in HLA-A*2402-restricted CMV-CTLs have not been clarified, even though HLA-A*2402 is the most common HLA-A allele in the Japanese population (~60%).

In this study, we investigated the TCR-β repertoire and clone monitoring of HLA-A*2402-restricted CMV-pp65$_{341–349}$ (QYDP-VAALF)-specific CTLs (CMV-pp65 CTLs) in Allo-HCT and found three distinct patterns of reconstitution for CMV-pp65 CTL clones.

PATIENTS AND METHODS

Patients and cells

This study included three pairs of recipients and their respective related donors. All of the recipients and donors were CMV-seropositive and had HLA-A*2402. The recipients received myeloablative conditioning using CY and TBI, and thereafter PBSC transplantation on day 0. Prophylaxis of GVHD was performed with CYA and short-term MTX. CMV reactivation was monitored weekly using a CMV antigenemia assay by the C10/11 method.

Peripheral blood samples were obtained from donors during the mobilization by G-CSF, whereas those from recipients were obtained every 1–3 months after Allo-HCT. Mononuclear cells were separated by density gradient sedimentation using Lymphoprep (Axis-Shield PoC AS, Dundee, Scotland) and were cryopreserved at −80 °C until use.

This study was approved by the institutional review board of Jichi Medical University and all subjects gave their written informed consent for the cryopreservation and analysis of the blood samples in accordance with the Helsinki declaration.

Staining and monitoring of HLA-A*2402-restricted CMV-pp65 CTLs

Cells were incubated with HLA-A*2402 CMV-pp65$_{341–349}$ peptide (QYDP-VAALF)-binding HLA tetramer (CMV tetramer) (Medical & Biological Laboratories, Nagoya, Japan), and then stained with anti-human CD3,

Division of Hematology, Saitama Medical Center, Jichi Medical University, Saitama, Japan. Correspondence: Dr Y Kanda, Division of Hematology, Saitama Medical Center, Jichi Medical University, 1-847, Amanuma-cho, Omiya-ku, Saitama 330-8503, Japan.
E-mail: ycanda-tky@umin.ac.jp
Received 6 March 2013; revised 19 April 2013; accepted 23 May 2013; published online 12 August 2013

CD8, CD4, CD14, CD16, CD19 and CD56 mAb (BD Biosciences, Tokyo, Japan). Data were analyzed with FACSCalibur and CellQuest (BD Biosciences). HLA-A*2402-restricted CMV-pp65 CTLs were defined as $CD8^+$CMV-tetramer$^+$ T cells. The proportions of CMV-pp65 CTLs to whole $CD8^+$ T cells were monitored every 1–3 months. We described the sampling phases as follows: the early phase, 1–3 months after Allo-HCT; the intermediate phase, about 6–9 months and the late phase, over 1 year after Allo-HCT.

Furthermore, phenotypic analysis was performed using non-cultured samples when sufficient CMV tetramer$^+$ T cells were detected for the first time after Allo-HCT and thereafter every 4–6 months: (Case-1) days 40, 215 and 376; (Case-2) days 58, 240 and 388; (Case-3) days 92, 264 and 416. Cells were incubated with CMV tetramer, and then stained with anti-human CD3, CD8, CD45RA and CCR7 mAbs (BD Biosciences). T cells were divided into four differentiation subsets according to their phenotypes: $CD45RA^+$ $CCR7^+$ naive T cell, $CD45RA^-CCR7^+$ central memory T (T_{CM}) cells, $CD45RA^-CCR7^-$effector-memory T (T_{EM}) cells and $CD45RA^+CCR7^-$ effector T (T_{EF}) cells.[6,13–15] Additionally, late-phase $CD8^+$CMV-tetramer$^+$ cells were also stained with CD27 and CD57 mAB (BD Biosciences). The maturation of T cells was defined according to the expression of CD27 and CD57:[16,17] $CD27^+CD57^-$immature T cells, $CD27^+CD57^+$, $CD27^-CD57^-$ T cells and $CD27^-CD57^+$mature T cells. Data were analyzed using FACSAria II and Diva software (BD Biosciences). The median absolute numbers of accepted CMV-tetramer-positive cells for phenotypic analysis were 639 cells (range:118–2157) in Case-1, 93 cells (range: 61–122) in Case-2 and 80 cells (range: 41–153) in Case-3, respectively (Supplementary Figure).

Single-cell TCR-β analysis of individual HLA-A*2402-restricted CMV-pp65 CTLs and clone monitoring

Clone identification by single-cell analysis was performed. The clone dynamics of each recipient was assessed using the same samples for phenotypic analysis. In Case-3, the proportions of CMV-tetramer$^+$ T cells were extremely low, and therefore samples on days 264 and 416 were combined with those on days 290 and 451, respectively. Thereafter, individual $CD3^+CD8^+$CMV-tetramer$^+$T cells were directly sorted as single cells into PCR tubes or microplates using FACSAria II (BD Biosciences). A median of 120 cells was sorted (range: 73–165) for each sample. The amino-acid (AA) sequences in CDR3 of TCR-β for sorted cells at a single-cell level were directly analyzed and determined after reverse transcript (RT)-PCR for TCR-β gene amplification as described previously.[11,12] In brief, individual CMV-pp65 tetramer$^+$ T cells were sorted at a single-cell level into PCR tubes. After direct cell lyses, cDNAs of TCR-β were synthesized by RT, with a TCR-β constant region gene-specific primer. The synthesized cDNA of TCR-β were used for two sequential steps of semi-nested PCR using 24 kinds of TCR-β variable region (BV) gene family-specific primers and two kinds of TCR-β constant primers. After we identified the BV family of individual cells, we directly sequenced AA of V-D-J CDR3 of T cells. The average efficiency of TCR analysis was 68: 77 in Case-1, 70 in Case-2 and 58% in Case-3.

Induction of CMV-pp65 CTLs in donor cells by culture in bulk

To compare the differences in the distribution of CMV-CTL clones between cultured and non-cultured cells, we cultured donor cells with 10 μg/mL of CMV-$pp65_{341–349}$ peptide (QYDPVAALF) (Sigma Genosys, Tokyo, Japan) in RPMI 1640 (Sigma, Tokyo, Japan) containing 10% fetal bovine serum (FBS). One day after peptide stimulation, 50 IU/mL of IL-2 (Shionogi, Osaka, Japan) were added to the medium. Thereafter, the medium was replaced with fresh medium that contained the same concentration of IL-2, as determined by the medium color. After 2 weeks, the cultured cells were collected and the repertoire of TCR-β in CMV-pp65 CTLs was analyzed as described above.

Establishment of a CMV-pp65 CTL clone from a single cell

To assess the cytotoxic effect of CMV-pp65 CTLs, CTL clones were established from the sample from Case-1 at 334 days after Allo-HCT. First, cells were cultured with 10 ng/mL of CMV-$pp65_{341–349}$ peptide in AIM-V (Life Technologies, Tokyo, Japan) with 10% human AB serum (Sigma). Two days after peptide stimulation, 50 IU/mL of IL-2 (Shionogi) were added. Thereafter, the medium was replaced with fresh medium that contained the same concentration of IL-2, as determined by the medium color. After 2 weeks, the cultured cells were collected and stained with CMV tetramer, anti-human CD3, CD8 and 7AAD mAbs (BD Biosciences). The $CD8^+$CMV-tetramer$^+$ T cells were sorted at a single-cell level into 96-well microplates with 100 μL/well of AIM-V containing 10% human AB serum, 5 μg/mL of PHA, 200 IU/mL of IL-2, and allo-feeder cells treated by mitomycin C. After 1 week, an additional 100 μL/well of AIM-V containing 10% human AB serum and 200 IU/mL of IL-2 were suspended in each well. After 4–6 weeks, cells were collected and we determined whether or not the proliferated cells were $CD8^+$CMV-tetramer$^+$ T cells. In Cases-2 and -3, CMV-pp65 CTL clones did not proliferate sufficiently.

Cytotoxicity of CMV-CTL clones

A fluorochromasia cytotoxicity assay was performed with a TERASCAN VPC system (Minerva Tech, Tokyo, Japan) according to previous reports.[18–20] Briefly, T2–24 cells that expressed HLA-A*2402 (kindly provided by Professor Kawakami of Keio University) were pulsed with 10 μg/mL of CMV-$pp65_{341–349}$ peptide (QYDPVAALF) or 10 μg/mL of HIV env gp 160 (RYLRDQQLL) (Sigma Genosys) for 1 h. The T2–24 cells as a target were then stained with calcein AM (WAKO, Osaka, Japan) for 30 min. After being washed three times, 1×10^4 T2–24 cells per well were suspended in a 96-well half area plate (Corning, Tokyo, Japan) and cultured with individual CMV-pp65 CTL clones in a dose-dependent manner. After 4 h, the release of calcein was measured and cytotoxicity was calculated.

RESULTS

Proportions and phenotypes of HLA-A*2402-restricted CMV-pp65 CTLs during the clinical courses

The patient backgrounds are shown in Table 1. Engraftment was successfully achieved in all three cases. Case-1 did not have CMV reactivation (Figure 1a). Case-1 experienced grade 2 acute GVHD and extensive chronic GVHD at 40 and 314 days after HCT, respectively. Although both the acute and chronic GVHD required steroid treatment, clinical CMV reactivation did not occur during the follow-up. Donor-1 showed a 0.66% CMV-pp65 CTLs, which included 67% $CD45RA^+CCR7^-T_{EF}$ and 27% $CD45RA^-CCR7^-$ T_{EM} cells (Figure 1b). The CMV-pp65 CTLs in the recipient appeared at 40 days after HCT and accounted for 5.2% of $CD8^+$ T cells. During the first 3 months, CMV-pp65 CTLs maintained a proportion of about 5% of $CD8^+$ T cells. Thereafter, the proportion of CMV-pp65 CTLs decreased, but remained at about 1–2% (Figure 1a). The proportion of $CD45RA^+CCR7^-T_{EF}$ cells in CMV-pp65 CTLs remained at 60–80% after Allo-HCT (Figure 1b).

Case-2 showed a CMV reactivation only in the early phase (Figure 1c). Case-2 did not experience acute GVHD, but developed

Table 1. Patient background

	Age		*Gender*		*Disease*	*CMV status*		*Conditioning*	*GVHD prophylaxis*	*CMV reactivation*
	Recipient	*Donor*	*Recipient*	*Donor*		*Recipient*	*Donor*			
Case-1	16	14	Male	Male	AML	+	+	CY-TBI	CsA + MTX	None
Case-2	36	33	Male	Male	AML	+	+	CY-TBI	CsA + MTX	Only in the early phase
Case-3	21	49	Male	Female	Acute promyelocytic leukemia	+	+	CY-TBI	CsA + MTX	Frequently

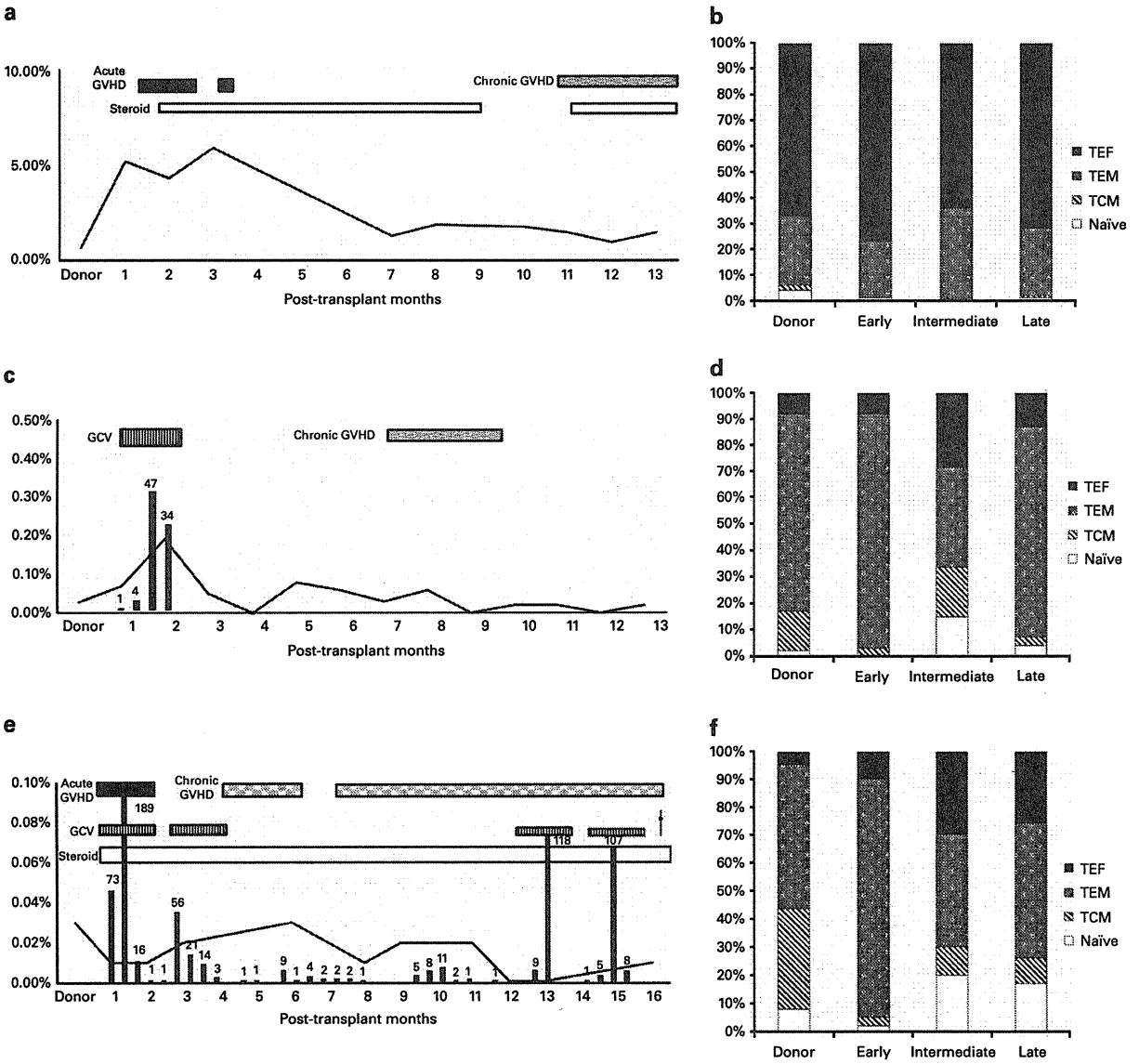

Figure 1. Clinical events and phenotypic dynamics of HLA-A*2402-restricted CMV-pp65-specific CTL (CMV-pp65 CTLs) in (**a** and **b**) Case-1, (**c** and **d**) Case-2 and (**e** and **f**) Case-3. (**a, c** and **e**) Clinical events and monitoring of the proportions of CMV-pp65 CTLs to whole CD8+ T cells; black vertical bars indicate CMV reactivation shown with counts of CMV antigenemia by the C10/11 method. (**b, d** and **f**) The dynamics of subpopulations of CMV-pp65 CTLs: CD45RA+CCR7+ naive T cells, CD45RA-CCR7+ central memory T cells (TCM), CD45RA-CCR7-effector-memory T cells (TEM) and CD45RA+CCR7-effector T cells (TEF). Early phase: days 40, 58 and 92; intermediate phase: days 215, 240 and 264; and late phase: days 376, 388 and 416 in Cases-1, -2 and -3, respectively.

limited chronic GVHD, which did not require steroid treatment. Donor-2 had 0.03% CMV-pp65 CTLs, almost all of which were $CD45RA^-CCR7^-$ T_{EM} cells (Figure 1d). Clinical CMV reactivation occurred 35 days after Allo-HCT and disappeared with GCV treatment. The CMV-pp65 CTLs accounted for 0.19% of $CD8^+$ T cells at 2 months after HCT. Thereafter, the proportion of CMV-pp65 CTLs decreased and remained at about 0.02–0.08% (Figure 1c). The CMV-pp65 CTLs after Allo-HCT included $CD45RA^+$ $CCR7^-$ T_{EF} cells, but most of the CMV-pp65 CTLs were $CD45RA^-$ $CCR7^-$ T_{EM} cells (Figure 1d).

Case-3 showed repeated CMV reactivation and experienced grade 4 acute GVHD and extensive chronic GVHD. He required long-term systemic steroid treatment (Figure 1e). Donor-3 had 0.03% CMV-pp65 CTLs in $CD8^+$ T cells. The CMV-pp65 CTLs included 52% $CD45RA^-CCR7^-T_{EM}$ and 36% $CD45RA^-CCR7^+$ T_{CM} cells, but few $CD45RA^+CCR7^-T_{EF}$ cells (Figure 1f). During follow-up, CMV-pp65 CTLs did not exceed 0.03% of $CD8^+$T cells (Figure 1e). The CMV-pp65 CTLs detected after Allo-HCT always included less $CD45RA^+CCR7^-T_{EF}$ cells than $CD45RA^-CCR7^-$ T_{EM} cells (Figure 1f).

Clonotypes of non-cultured HLA-A*2402-restricted CMV-pp65 CTLs

The clonotypes of CMV-pp65 CTLs were assessed in a total of 993 cells: 330 cells in Case-1, 335 cells in Case-2 and 268 cells in Case-3. BV7 were used among the BV family in 21, 16 and 35% of CMV-pp65 CTLs in Cases-1, -2 and -3, respectively. In addition, BJ1-1 was used among the BJ family in 21, 35 and 26% of CMV-pp65 CTLs in Cases-1, -2 and -3, respectively (Figure 2).

Of the total 993 cells, 187 clones were identified: 30, 74 and 83 in Cases-1, -2 and -3, respectively. Table 2 shows the features of clones that appeared in three or more cells during the follow-up. Within each case, specific AA sequences of CDR3 were found: DPG in Case-1, GQG and PRD in Case-2, and QVS in Case-3. Although no common AA motif of CDR3 was found among the three cases, GGGG was seen in the dominant clones in both Cases-1 and -3 (Table 2).

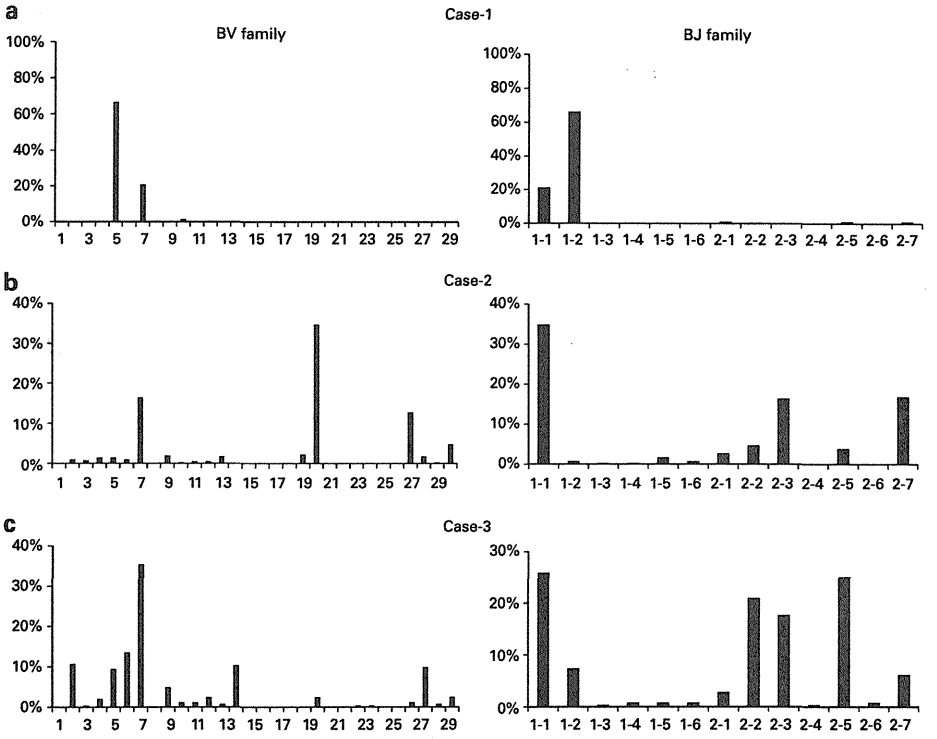

Figure 2. BV and BJ gene usages in HLA-A*2402-restricted CMV-pp65-specific cytotoxic T cells observed in (**a**) Case-1, (**b**) Case-2 and (**c**) Case-3.

Table 2. *Clonotypes of CDR3 of TCR-β in HLA-A*2402-restricted CMV-specific CTLs, which appeared in three or more cells during follow-up*

Case	*Clone-ID*	*Number of cells*	*BV*	*Amino acid of CDR3*	*BJ*
Case-1 (330 cells)	N-1	231	BV5	CASS**DPG**DSLNGYTF	BJ1-1
	N-2	66	BV7	CASS*STGGGG*TEAFF	BJ1-1
	N-9	6	BV10	CAIS**DPG**HRFGEAFF	BJ1-1
Case-2 (335 cells)	S-1	128	BV20	CSARFS**GQG**TEAFF	BJ1-1
	S-2	50	BV7	CASSSNQGATQYF	BJ2-3
	S-3	7	BV13	CASINRGTDPYEQYF	BJ2-7
	S-4	42	BV27	CAST**PRD**RSNYEQYF	BJ2-7
	S-7	9	BV7	CASSFTLSPETQYF	BJ2-5
	S-24	3	BV4	CASSQ**GQG**AQNQPQHF	BJ1-5
	S-32	18	BV30	CAGTGIRSAGELFF	BJ2-2
	S-56	4	BV28	CASK**PRD**SGDTQYF	BJ2-3
	S-57	3	BV20	CSARNPGLYEQYF	BJ2-7
Case-3 (268 cells)	I-1	18	BV7	CASSSIQGAAGELFF	BJ2-2
	I-2	24	BV14	CASS**QVS**TGETQYF	BJ2-5
	I-3	20	BV2	CASRG**QVS**SQETQYF	BJ2-5
	I-4	3	BV2	CAIKGTVSTQETQYF	BJ2-5
	I-24	50	BV7	CASSST*GGGG*AEAFF	BJ1-1
	I-25	25	BV6	CASDRGGNTGELFF	BJ2-2
	I-26	8	BV5	CASSLDTDTQYF	BJ2-3
	I-27	10	BV28	CASSPDRGRGYTF	BJ1-2
	I-28	7	BV7	CASSLSSTRTDTQYF	BJ2-3
	I-29	7	BV28	CASSLNSVGTEAFF	BJ1-1
	I-30	3	BV28	CASSSDNAIGGGSYGYTF	BJ1-2
	I-32	8	BV5	CASSLGAGGPSDTQYF	BJ2-3
	I-34	3	BV7	CASSLGGLAPSTDTQYF	BJ2-3

Abbreviations: BV = TCR-β variable region; CDR3 = complementarity-determining region 3; TCR = T-cell receptor. Bold letters indicate shared motifs of CDR3 within each case. Italic letters indicate a shared motif of CDR3 between Case-1 and Case-3.

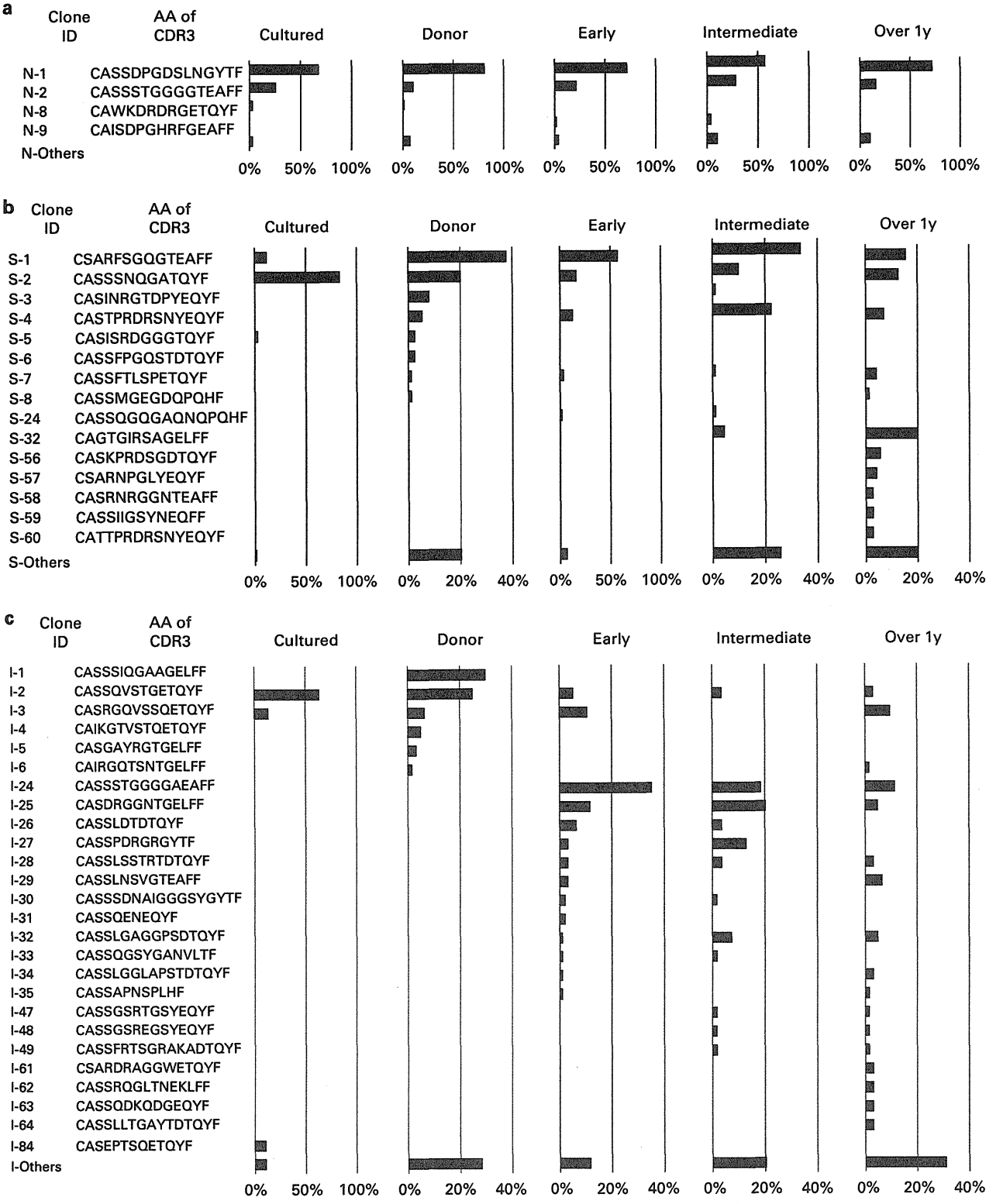

Figure 3. Clone monitoring of HLA-A*2402-restricted CMV-pp65-specific cytotoxic T cells in donors and recipients in the early, intermediate and late phases. Clones, which appeared at two or more points/two or more clones at one point, are shown with the clone-ID and amino acid (AA) sequences of CDR3 of T-cell receptor-β in (**a**) Case-1, (**b**) Case-2 and (**c**) Case-3. In addition, clones of cultured donor cells were also shown. Early phases: days 40, 58 and 92; intermediate phase: days 215, 240 and 264 and 290; and late phase: days 376, 388 and 416 and 451 in Cases-1, -2 and -3, respectively.

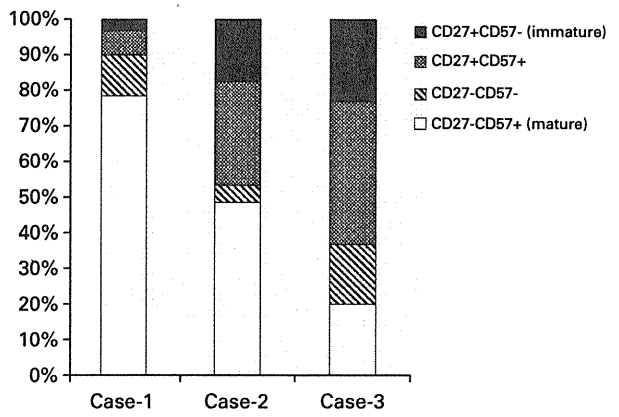

Figure 4. Maturation of HLA-A*2402-restricted CMV-pp65 CTLs among cases.

Clone monitoring of HLA-A*2402-restricted CMV-pp65 CTLs

Serial clone monitoring was performed using non-cultured donor cells, and recipient cells of early, intermediate and late phases (Figures 3a–c). In Case-1, who did not show CMV reactivation during the follow-up, the dominant CMV-pp65 CTL clones in the donor were well preserved in the recipient after Allo-HCT (Figure 3a). Especially, clone N-1 with CAISDPGHRFGEAFF of CDR3-AA always exceeded 50% in Case-1. Few novel clones (<10%) appeared during the follow-up.

In Case-2, who developed CMV reactivation only within the early phase after HCT, the dominant CMV-CTL clones in the donor were preserved in the early phase after Allo-HCT. However, novel clones appeared and gradually became dominant in a later phase (Figure 3b). At any point, at least one clone exceeded 20%.

In Case-3, who showed repeated CMV reactivation, some of the donor-dominant CMV-CTL clones were preserved in the early phase, but the novel clone I-24 with CASSSTGGGGAEAFF was the most dominant in the early phase (Figure 3c). However, the clones became more diverse during the follow-up, and eventually none of the clones exceeded 20% in the later phase.

The maturation analysis was also performed using samples of the later phase. $CD27^-CD57^+$ mature T cells accounted for 80% of the CMV-pp65 CTLs in Case-1, in whom donor-dominant clones remained dominant. On the other hand, the amount of $CD27^+$ immature T cells was increased in Cases-2 and -3, both of whom showed novel clones (Figure 4).

Difference in HLA-A*2402-restricted CMV-pp65 CTL clones between cultured and non-cultured cells in respective donors

CMV-pp65 CTL clones were compared between cultured and non-cultured cells of the donors. In Case-1, the dominant clones in cultured cells were detected in non-cultured cells and the proportions of dominant clones were similar (Figure 3a). However, in both Cases-2 and -3, the proportions of dominant CMV-pp65 CTLs were different between cultured and non-cultured cells, especially in Case-3 (Figures 3b and c).

Cytotoxicity

Two clones were established from Case-1: the most dominant clone N-1 with CASSDPGDSLNGYTF of CDR3, and clone N-X with CASSLSGVDYNEQFF, which was not detected by single-cell analysis at any point. Both clone N-1 and clone N-X showed specific cytotoxicity against CMV-pp65 in a dose-dependent manner. The dominant clone N-1 exhibited 53 and 70% of cytotoxicity at the E:T ratio of 1.25 and 5, respectively. On the other hand, the minor clone N-X exhibited 20 and 30% of cytotoxicity at the corresponding E:T ratios (Figures 5a and b).

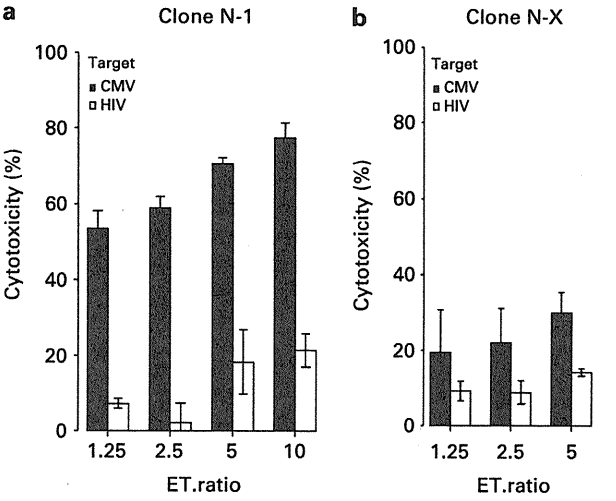

Figure 5. Cytotoxicity assay for clones of HLA-A*2402-restricted CMV-pp65-specific cytotoxic T cells. Two clones were established from Case-1: (**a**) the most dominant clone N-1, with CASSDPGDSLNGYTF of TCR-β CDR3, and (**b**) clone N-X, with CASSLSGVDYNEQFF, which was not found at any point.

DISCUSSION

Using a direct single-cell analysis of the TCR-β repertoire, we conducted clone monitoring of CMV-pp65 CTLs in three donor–recipient pairs of Allo-HCT and analyzed about 1000 cells. The methods enabled the simultaneous identification and quantification of CTL clones and we could visualize the *in vivo* dynamics of CMV-pp65 CTL clones without *in vitro* expansion, which may affect the proportions of CTL clones.

To date, various studies have investigated CMV-specific CTLs[6–10,16,21,22] and reconstitution after Allo-HCT.[5,23–32] However, neither flow cytometry using a panel of mAbs to the TCR-BV family[7,9,27] nor TCR-BV spectratyping[7,10] could reflect the dynamics of CMV-CTLs at a clone level. Furthermore, *in vitro* culture and bacterial transformation are required in a clonotype-specific PCR method, which has been used to identify and quantify CMV-CTL clones.[7,8,30] Therefore, it might result in a biased selection of CTL clones according to their proliferative potential.[33,34] In fact, we observed differences in dominant clones between cultured and non-cultured donor cells in Cases-2 and -3. The current direct single-cell analysis method is important for evaluating the *in vivo* dynamics of CMV-CTL more precisely.

To the best of our knowledge, this study is the first to describe the comprehensive dynamics and monitoring of CMV-pp65 CTL clones after Allo-HCT. We investigated the clone dynamics in three distinct patterns of CMV reactivation: (1) no CMV reactivation, (2) CMV reactivation only within the early phase and (3) repeated CMV reactivation. Like the results in previous studies,[30,35] several CMV-pp65 CTL clones in the donors were actually detected in the recipients after Allo-HCT. Especially in Case-1 without CMV reactivation, dominant clones of Donor-1 persisted and remained dominant even after Allo-HCT, which might reflect a high proportion of CD27-CD57+ mature CMV-pp65 CTLs in Case-1 at 1 year after Allo-HCT. On the other hand, not all of the clones detected in the recipients after Allo-HCT were present in their corresponding donors. Furthermore, we found that dominant clones in a donor were not always dominant in a recipient after Allo-HCT. In Cases-2 and -3 with CMV reactivation, novel clones appeared and became dominant during the follow-up. The emergence of novel clones might be associated with more CD27+ immature CMV-pp65 CTLs at 1 year after Allo-HCT, especially in Case-3.

The cellular response to CMV is known to be frequently impaired and CMV reactivation often occurs in recipients of solid organ transplant or Allo-HCT, even in the presence of CMV-CTL.[21,26] However, in Case-1, CMV reactivation did not occur despite the long-term use of systemic steroid. One possible explanation for this finding may be the protective phenotype of CMV-CTLs in this patient, compared with those in the other two patients. In Case-1, CMV-pp65 CTLs included about 70% of highly differentiated $CD45RA^+CCR7^-$ T_{EF} cells during follow-up, whereas this value was $<30\%$ in the other two patients. Cytokine production and cytotoxicity are known to increase in association with differentiation, and $CD45RA^+CCR7^-$ T_{EF} cells are believed to have high killing potential.[14,15] The clinical course of CMV reactivation might be affected by the phenotype of CMV-CTLs in the recipients after HCT.

It remains a matter of debate which is important for eliminating infectious pathogens, TCR diversity or selected clones with high avidity.[36] In the previous report, TCR diversity was linked to host resistance against viral infection.[37] On the other hand, another report suggested that TCR diversity had no functional advantage on CTL response.[38] In the current study, Case-1 with highly selected clones seemed to have more advantages on CMV reactivation than Case-3 with more diverse repertoire, although this study is too small to draw a conclusion. Further investigation is necessary to address this issue in allo-HCT recipients.

In previous reports on healthy subjects with HLA-A2 or HLA-B7, dominant clones selected specific BV and BJ genes, and had a particular common AA motif of TCR-β CDR3 in unrelated subjects.[9] In the current study, HLA-A*2402-restricted CMV-pp65 CTLs tended to select BV7 and BJ1-1. Although no common AA motif was found among the cases, GGGG was present in dominant clones in two cases. A larger study will be required to show whether a common motif exists in allo-HCT recipients. Effective immune reconstitution is critical to control CMV reactivation before it progresses to CMV diseases such as pneumonia or colitis, which have high mortality rates.[1–4] Gauging the TCR repertoire and identifying most effective clonotypes of CMV-CTLs may lead to a specific immunotherapy against treatment-refractory CMV infection, as in anticancer therapy.[39]

This study had several limitations and challenges regarding the methodology. First, our study included only three donor–patient pairs, although the clonotypes of about 1000 cells were analyzed. Therefore, we could not form any definite conclusions regarding the association between clinical CMV reactivation and the dynamics of CMV-pp65 CTL clones.[26,28–30] Second, it should be noted that the proportion of HLA-A*2402-restricted CMV-CTLs was quite low at later time points, especially in Case-3. Phenotypic analysis might be susceptible to the low number. Third, clones of CMV-pp65 CTLs in Cases-2 and -3 could not be established by the current experimental methods. This may have been due to the exposure to steroid or GVHD. To compare the cytotoxicities and cytokine production of CMV-pp65 CTL clones, a method that enables sufficient cell proliferation from a single cell will need to be established.

In summary, we focused on the reconstitution of HLA-A*2402-restricted CMV-pp65 CTLs following allo-HCT, and performed clone monitoring using a single-cell analysis method. HLA-A*2402-restricted CMV-pp65 CTLs tended to select BV7 and BJ1-1. The phenotypes and *in vivo* dynamics of CMV-pp65 CTLs differed according to three distinct patterns of CMV reactivation. A larger study is warranted to assess the association between CMV reactivation and reconstitution patterns of CMV-CTLs. *In vivo* clone monitoring of CMV-CTLs could provide insight into the mechanism of immunological reconstitution following allo-HCT.

CONFLICT OF INTEREST

The authors declare no conflict of interest.

ACKNOWLEDGEMENTS

This study was supported in part by a Health and Labor Science Research Grant (Research on Allergic Disease and Immunology) from the Ministry of Health, Labour and Welfare of Japan (YK). We would also like to express our appreciation for the support of JKA through its promotion funds from KEIRIN RACE.

AUTHOR CONTRIBUTIONS

HN designed the study, performed the experiments, analyzed data and wrote the manuscript. YT and R Yamazaki, designed the study and gave their advice about the experimental procedures. MS, KT, KS, R Yamasaki, HW, YI, KK, TM, MA, Shun-ichi K, MK, AT, JK, Shinichi K and JN collected data. YK designed the study, analyzed data and wrote the manuscript.

REFERENCES

1 Stocchi R, Ward KN, Fanin R, Baccarani M, Apperley JF. Management of human cytomegalovirus infection and disease after allogeneic bone marrow transplantation. *Haematologica* 1999; **84**: 71–79.
2 Mori T, Kato J. Cytomegalovirus infection/disease after hematopoietic stem cell transplantation. *Int J Hematol* 2010; **91**: 588–595.
3 Ljungman P, Engelhard D, Link H, Biron P, Brandt L, Brunet S *et al.* Treatment of interstitial pneumonitis due to cytomegalovirus with ganciclovir and intravenous immune globulin: experience of European Bone Marrow Transplant Group. *Clin Infect Dis* 1992; **14**: 831–835.
4 Ljungman P, Brand R, Einsele H, Frassoni F, Niederwieser D, Cordonnier C. Donor CMV serologic status and outcome of CMV-seropositive recipients after unrelated donor stem cell transplantation: an EBMT megafile analysis. *Blood* 2003; **102**: 4255–4260.
5 Moins-Teisserenc H, Busson M, Scieux C, Bajzik V, Cayuela JM, Clave E *et al.* Patterns of cytomegalovirus reactivation are associated with distinct evolutive profiles of immune reconstitution after allogeneic hematopoietic stem cell transplantation. *J Infect Dis* 2008; **198**: 818–826.
6 Gamadia LE, Rentenaar RJ, Baars PA, Remmerswaal EB, Surachno S, Weel JF *et al.* Differentiation of cytomegalovirus-specific CD8(+) T cells in healthy and immunosuppressed virus carriers. *Blood* 2001; **98**: 754–761.
7 Wynn KK, Fulton Z, Cooper L, Silins SL, Gras S, Archbold JK *et al.* Impact of clonal competition for peptide-MHC complexes on the CD8+ T-cell repertoire selection in a persistent viral infection. *Blood* 2008; **111**: 4283–4292.
8 Babel N, Brestrich G, Gondek LP, Sattler A, Wlodarski MW, Poliak N *et al.* Clonotype analysis of cytomegalovirus-specific cytotoxic T lymphocytes. *J Am Soc Nephrol* 2009; **20**: 344–352.
9 Day EK, Carmichael AJ, ten Berge IJ, Waller EC, Sissons JG, Wills MR. Rapid CD8+ T cell repertoire focusing and selection of high-affinity clones into memory following primary infection with a persistent human virus: human cytomegalovirus. *J Immunol* 2007; **179**: 3203–3213.
10 Peggs K, Verfuerth S, Pizzey A, Ainsworth J, Moss P, Mackinnon S. Characterization of human cytomegalovirus peptide-specific CD8(+) T-cell repertoire diversity following *in vitro* restimulation by antigen-pulsed dendritic cells. *Blood* 2002; **99**: 213–223.
11 Tanaka-Harada Y, Kawakami M, Oka Y, Tsuboi A, Katagiri T, Elisseeva OA *et al.* Biased usage of BV gene families of T-cell receptors of WT1 (Wilms' tumor gene)-specific CD8+ T cells in patients with myeloid malignancies. *Cancer Sci* 2010; **101**: 594–600.
12 Tanaka Y, Nakasone H, Yamazaki R, Sato K, Sato M, Terasako K *et al.* Single-cell analysis of T-cell receptor repertoire of HTLV-1 Tax-specific cytotoxic T cells in allogeneic transplant recipients with adult T-cell leukemia/lymphoma. *Cancer Res* 2010; **70**: 6181–6192.
13 Sallusto F, Lenig D, Forster R, Lipp M, Lanzavecchia A. Two subsets of memory T lymphocytes with distinct homing potentials and effector functions. *Nature* 1999; **401**: 708–712.
14 Koch S, Larbi A, Ozcelik D, Solana R, Gouttefangeas C, Attig S *et al.* Cytomegalovirus infection: a driving force in human T cell immunosenescence. *Ann N Y Acad Sci* 2007; **1114**: 23–35.
15 Sallusto F, Geginat J, Lanzavecchia A. Central memory and effector memory T cell subsets: function, generation, and maintenance. *Annu Rev Immunol* 2004; **22**: 745–763.
16 Kern F, Khatamzas E, Surel I, Frommel C, Reinke P, Waldrop SL *et al.* Distribution of human CMV-specific memory T cells among the CD8pos. subsets defined by CD57, CD27, and CD45 isoforms. *Eur J Immunol* 1999; **29**: 2908–2915.
17 Appay V, Dunbar PR, Callan M, Klenerman P, Gillespie GM, Papagno L *et al.* Memory CD8+ T cells vary in differentiation phenotype in different persistent virus infections. *Nat Med* 2002; **8**: 379–385.

18 Muneta Y, Nagaya H, Minagawa Y, Enomoto C, Matsumoto S, Mori Y. Expression and one-step purification of bovine interleukin-21 (IL-21) in silkworms using a hybrid baculovirus expression system. *Biotechnol Lett* 2004; **26**: 1453–1458.
19 Sasawatari S, Tadaki T, Isogai M, Takahara M, Nieda M, Kakimi K. Efficient priming and expansion of antigen-specific CD8+ T cells by a novel cell-based artificial APC. *Immunol Cell Biol* 2006; **84**: 512–521.
20 Motomura Y, Ikuta Y, Kuronuma T, Komori H, Ito M, Tsuchihara M *et al.* HLA-A2 and -A24-restricted glypican-3-derived peptide vaccine induces specific CTLs: preclinical study using mice. *Int J Oncol* 2008; **32**: 985–990.
21 Engstrand M, Lidehall AK, Totterman TH, Herrman B, Eriksson BM, Korsgren O. Cellular responses to cytomegalovirus in immunosuppressed patients: circulating CD8+ T cells recognizing CMVpp65 are present but display functional impairment. *Clin Exp Immunol* 2003; **132**: 96–104.
22 Kuzushima K, Hayashi N, Kimura H, Tsurumi T. Efficient identification of HLA-A*2402-restricted cytomegalovirus-specific CD8(+) T-cell epitopes by a computer algorithm and an enzyme-linked immunospot assay. *Blood* 2001; **98**: 1872–1881.
23 Reusser P, Riddell SR, Meyers JD, Greenberg PD. Cytotoxic T-lymphocyte response to cytomegalovirus after human allogeneic bone marrow transplantation: pattern of recovery and correlation with cytomegalovirus infection and disease. *Blood* 1991; **78**: 1373–1380.
24 Walter EA, Greenberg PD, Gilbert MJ, Finch RJ, Watanabe KS, Thomas ED *et al.* Reconstitution of cellular immunity against cytomegalovirus in recipients of allogeneic bone marrow by transfer of T-cell clones from the donor. *N Engl J Med* 1995; **333**: 1038–1044.
25 Cwynarski K, Ainsworth J, Cobbold M, Wagner S, Mahendra P, Apperley J *et al.* Direct visualization of cytomegalovirus-specific T-cell reconstitution after allogeneic stem cell transplantation. *Blood* 2001; **97**: 1232–1240.
26 Ozdemir St E, John LS, Gillespie G, Rowland-Jones S, Champlin RE, Molldrem JJ *et al.* Cytomegalovirus reactivation following allogeneic stem cell transplantation is associated with the presence of dysfunctional antigen-specific CD8+ T cells. *Blood* 2002; **100**: 3690–3697.
27 Lacey SF, Gallez-Hawkins G, Crooks M, Martinez J, Senitzer D, Forman SJ *et al.* Characterization of cytotoxic function of CMV-pp65-specific CD8+ T-lymphocytes identified by HLA tetramers in recipients and donors of stem-cell transplants. *Transplantation* 2002; **74**: 722–732.
28 Hebart H, Daginik S, Stevanovic S, Grigoleit U, Dobler A, Baur M *et al.* Sensitive detection of human cytomegalovirus peptide-specific cytotoxic T-lymphocyte responses by interferon-gamma-enzyme-linked immunospot assay and flow cytometry in healthy individuals and in patients after allogeneic stem cell transplantation. *Blood* 2002; **99**: 3830–3837.
29 Mohty M, Mohty AM, Blaise D, Faucher C, Bilger K, Isnardon D *et al.* Cytomegalovirus-specific immune recovery following allogeneic HLA-identical sibling transplantation with reduced-intensity preparative regimen. *Bone Marrow Transplant* 2004; **33**: 839–846.
30 Scheinberg P, Melenhorst JJ, Brenchley JM, Hill BJ, Hensel NF, Chattopadhyay PK *et al.* The transfer of adaptive immunity to CMV during hematopoietic stem cell transplantation is dependent on the specificity and phenotype of CMV-specific T cells in the donor. *Blood* 2009; **114**: 5071–5080.
31 Moss P, Rickinson A. Cellular immunotherapy for viral infection after HSC transplantation. *Nat Rev Immunol* 2005; **5**: 9–20.
32 Morita Y, Hosokawa M, Ebisawa M, Sugita T, Miura O, Takaue Y *et al.* Evaluation of cytomegalovirus-specific cytotoxic T-lymphocytes in patients with the HLA-A*02 or HLA-A*24 phenotype undergoing hematopoietic stem cell transplantation. *Bone Marrow Transplant* 2005; **36**: 803–811.
33 Zhou J, Dudley ME, Rosenberg SA, Robbins PF. Selective growth, *in vitro* and *in vivo,* of individual T cell clones from tumor-infiltrating lymphocytes obtained from patients with melanoma. *J Immunol* 2004; **173**: 7622–7629.
34 thor Straten P, Kirkin AF, Siim E, Dahlstrom K, Drzewiecki KT, Seremet T *et al.* Tumor infiltrating lymphocytes in melanoma comprise high numbers of T-cell clonotypes that are lost during *in vitro* culture. *Clin Immunol* 2000; **96**: 94–99.
35 Gandhi MK, Wills MR, Okecha G, Day EK, Hicks R, Marcus RE *et al.* Late diversification in the clonal composition of human cytomegalovirus-specific CD8+ T cells following allogeneic hemopoietic stem cell transplantation. *Blood* 2003; **102**: 3427–3438.
36 Turner SJ, La Gruta NL, Kedzierska K, Thomas PG, Doherty PC. Functional implications of T cell receptor diversity. *Curr Opin Immunol* 2009; **21**: 286–290.
37 Messaoudi I, Guevara Patiño JA, Dyall R, LeMaoult J, Nikolich-Zugich J. Direct link between mhc polymorphism, T cell avidity, and diversity in immune defense. *Science* 2002; **298**: 1797–1800.
38 La Gruta NL, Thomas PG, Webb AI, Dunstone MA, Cukalac T, Doherty PC *et al.* Epitope-specific TCR-β repertoire diversity imparts no functional advantage on the CD8+ T cell response to cognate viral peptides. *Proc Natl Acad Sci USA* 2008; **105**: 2034–2039.
39 Merhavi-Shoham E, Haga-Friedman A, Cohen CJ. Genetically modulating T-cell function to target cancer. *Semin Cancer Biol* 2012; **22**: 14–22.

Supplementary Information accompanies this paper on Bone Marrow Transplantation website (http://www.nature.com/bmt)

Biol Blood Marrow Transplant 19 (2013) 1013–1020

Biology

Allotype Analysis to Distinguish the Origin of Varicella-Zoster Virus Immunoglobulin G after Allogeneic Stem Cell Transplantation

Rie Yamazaki, Hideki Nakasone, Yukie Tanaka, Miki Sato, Kiriko Terasako, Hidenori Wada, Yuko Ishihara, Koji Kawamura, Kana Sakamoto, Masahiro Ashizawa, Tomohito Machishima, Shun-ichi Kimura, Misato Kikuchi, Shinya Okuda, Shinichi Kako, Junya Kanda, Aki Tanihara, Junji Nishida, Yoshinobu Kanda*

Division of Hematology, Department of Internal Medicine, Saitama Medical Center, Jichi Medical University, Saitama, Japan

Article history:
Received 4 March 2013
Accepted 5 April 2013

Key Words:
Immunoglobulin G allotype
Varicella-Zoster virus
Allogeneic stem cell transplantation
Humoral immunity

A B S T R A C T

Varicella-zoster virus (VZV) reactivation is a frequent complication after allogeneic hematopoietic stem cell transplantation (HSCT). Although previous studies have revealed that cellular immunity is important for suppressing reactivation, the role of humoral immunity against VZV has been poorly evaluated. We analyzed inherited polymorphisms in the immunoglobulin G (IgG) heavy chain constant regions of 50 HSCT recipient-donor pairs to distinguish donor-derived and recipient-derived antibodies. Twelve pairs were informative regarding the origin of IgG, since either the donors (n = 3) or recipients (n = 9) were homozygous null for the IgG1m(f) allotype. In these 9 homozygous-null recipients, allotype-specific IgG against VZV were measured by enzyme-linked immunosorbent assay and compared with measles-IgG. All 9 homozygous-null recipients were monitored for more than 1 year after HSCT, with (n = 4, localized zoster) or without (n = 5) clinical VZV disease. In 3 patients with VZV disease, donor-derived IgG against VZV was elevated between 500 to 700 days after HSCT after the episode of VZV disease. In 1 patient who suffered from VZV disease just before HSCT, donor-derived VZV IgG was elevated within 3 months after HSCT. On the other hand, 2 patients who received reduced-intensity conditioning (RIC) transplantation from an IgG1m(f) null donor maintained recipient-derived IgG against VZV for more than 1 year, whereas it was decreased within 3 months in 1 recipient who received conventional conditioning. In conclusion, the production of anti-VZV IgG by recipient plasma cells persists long after RIC. In patients without symptomatic VZV reactivation, donor-derived anti-VZV IgG did not reach titers comparable to those measured in healthy virus carriers.

BACKGROUND

Varicella-zoster virus (VZV) reactivation is a frequent complication after allogeneic hematopoietic stem cell transplantation (HSCT). It is sometimes disseminated and results in high mortality [1-3]. The incidence of VZV reactivation within 1 year after autologous and allogeneic HSCT ranges from 13% to 55% [3]. In a retrospective study of 100 consecutive allogeneic HSCT patients, 41% developed a VZV infection at a median of 227 (45 to 346) days after HSCT [2]. Tomonari et al. reported that the cumulative incidence of VZV reactivation after cord blood transplantation (CBT) was 80% [4]. This extremely high incidence might result from the immature nature of cord blood lymphocytes.

Many previous studies have shown that cellular immunity is important for suppressing VZV reactivation [5-9]. VZV memory T cells can usually be detected by 9 to 12 months after HSCT and are correlated with a reduction in the risk and complications of VZV disease [6]. The reconstitution of cellular immunity against VZV can be achieved by a subclinical episode of reactivation documented by PCR [7].

On the other hand, the role of humoral immunity against VZV has been poorly evaluated, including the presence of donor-derived or recipient-derived VZV IgG after allogeneic HSCT. Inherited polymorphisms in IgG heavy chain constant regions can be recognized by allotype-specific monoclonal antibodies and, thus, can be used to distinguish donor and recipient antibodies [10]. In the present study, we determined inherited polymorphisms in an IgG allotype, IgG1m(f), in 50 HSCT donor-recipient pairs and evaluated the status of donor-derived and recipient-derived VZV IgG production in 12 informative pairs using enzyme-linked immunosorbent assay (ELISA).

PATIENTS AND METHODS

Patients and HSCT Protocol

Fifty patients who underwent allogeneic HSCT at our institution from March 2008 to April 2011 and who were followed up for at least 1 year were evaluated in this study. The conventional conditioning regimen was mainly a combination of cyclophosphamide (60 mg/kg for 2 days) and total body irradiation (TBI, 2 Gy twice daily for 3 days) (n = 26). The reduced-intensity conditioning (RIC) regimen was mainly fludarabine combined with melphalan (±low-dose TBI, n = 14), cyclophosphamide and TBI (±ATG, n = 5), busulfan (±low-dose TBI, n = 4), or only low-dose TBI (n = 1). Standard graft-versus-host disease (GVHD) prophylaxis consisted of the continuous infusion of cyclosporine with a starting dose of 3 mg/kg/day and short-term methotrexate. Each patient provided written informed consent to be enrolled in the study. This study was approved by the Institutional Review Board of Jichi Medical University.

Financial disclosure: See Acknowledgments on page 1019.

* Correspondence and reprint requests: Yoshinobu Kanda, PhD, MD, Division of Hematology, Department of Internal Medicine, Saitama Medical Center, Jichi Medical University, 1-847 Amanuma, Omiya-ku, Saitama-city, Saitama 330-8503, Japan.
E-mail address: ycanda-tky@umin.ac.jp (Y. Kanda).

1083-8791/$ – see front matter © 2013 American Society for Blood and Marrow Transplantation.
http://dx.doi.org/10.1016/j.bbmt.2013.04.007

Prophylactic Administration of Acyclovir

Acyclovir (ACV) was routinely used as prophylaxis against herpes simplex virus infection from days -7 to 35. A long-term administration of low-dose ACV (200 mg/day) for VZV reactivation was started continuously on day 36 as described previously [11]. ACV was discontinued while ganciclovir or foscarnet was administered for the treatment of cytomegalovirus infection. ACV administration was continued for at least 1 year after HSCT or longer in patients who were persistently treated with immunosuppressants.

Diagnosis and Treatment of VZV Disease

The diagnosis of VZV disease was made by the presence of characteristic vesicular skin lesion on an erythematous base within a dermatome or a generalized cutaneous distribution. Microbiological and pathological conformation was not performed because all cases develop with typical skin lesions. VZV disease was treated with oral valacyclovir at 3 g/day for 7 days.

ELISA for the IgG Allotype

Plasma specimens of 50 recipients and 20 related donors were available for IgG allotype testing using an ELISA assay. The 1:2000-diluted mouse monoclonal antibodies specific for the G1m(f) allotype (I5385; Sigma, St. Louis, MO) were coated overnight at 4°C on a 96-well microtiter plate (Nunc-Immuno Plate, PolySorp, Thermo Fisher Scientific, Rochester, NY). After the wells were blocked with 200 microliters (μL) of phosphate-buffered saline with 2% fetal bovine serum for 1 hour, 1:1000-diluted plasma samples were incubated in duplicate under continuous shaking at room temperature for 2 hours. After 3 washes, 1:2000-diluted peroxidase-conjugated rabbit anti-human IgG whole molecule (Sigma) was added and incubated for 1 hour at room temperature. After 3 washes, 100 μL of an ABTS peroxidase substrate system (KPL, Gaithersburg, MD) was added to each well and the plate was read with a plate reader at 405 nanometers (nm). The results were evaluated conveniently by a cut-off index (COI). The COI was calculated as the mean OD^{405} from a sample divided by the cut-off value that was defined as the mean OD^{405} of 5 negative controls plus the 2-fold standard deviation. This assay was repeated to evaluate the timing of the appearance of donor-derived IgG or the disappearance of recipient-derived IgG in 12 allotype-informative patients.

Genotyping

Because plasma samples for ELISA were not available from unrelated donors, we speculated donor allotype based on the results of ELISA using the recipients' plasma samples before and after HSCT. If the recipients were IgG1m(f)-negative before HSCT (n = 24), the allotype of their donors could be determined as IgG1m(f)-positive when they became IgG1m(f)-positive after HSCT. However, if the recipients were IgG1m(f)-positive before HSCT (n = 6), it was impossible to determine the allotype of their donors. Therefore, for unrelated donors with IgG1m(f)-positive recipients, the genotyping of human immunoglobulin heavy chain allotype was carried out as described previously [12,13] to determine the donor allotype. Genomic DNA was isolated from post-HSCT patients' peripheral blood after complete donor chimerism was achieved, with a DNA mini kit (QIAGEN, Valencia, CA). Oligonucleotides PR1 (5′ CCCCTGGCACCCTCCTCCAA 3′) and PR2 (5′ GCCCTGGACTGGGGCTGCAT 3′) were used as the primer set for the amplification of a 364-base pair fragment from the constant region domain of the human IgG1 heavy chain. The conditions for PCR amplification were 94°C for 2 minutes followed by 30 cycles of 96°C for 1 minute, 70°C for 30 seconds, 72°C for 1 minute, and, finally, 7 minutes of incubation at 72°C. The total volume of the PCR mixture was 50 μL, containing 1 μL of genomic DNA, 1 mM $MgCl_2$, 5 units of Platinum taq DNA polymerase, .2 mM dNTP mix, and .2 μM of each primer. After the reaction products were separated by 2% agarose gel electrophoresis and single bands were confirmed, all of the PCR products were purified using a QIAquick PCR Purification kit (QIAGEN) and sequenced in forward directions using an ABI 3700 instrument and a BigDye sequencing kit (Applied Biosystems, Foster City, CA). IgG1m(f) allotypes included arginine residues instead of lysine at position 214 in the γ1 chain of immunoglobulins. This amino acid difference is due to a single base substitution in the coding DNA (A or G). Meanwhile, homozygous A of this single nucleotide polymorphism indicates IgG1m(f) allotype negative; that is, allotype of IgG1m(z). Heterozygous G, heterozygous A, or homozygous G indicates IgG1m(f) allotype positive.

Measurement of VZV-Specific and Measles-Specific IgG after HSCT

Frozen plasma from before HSCT and 6 and 12 months after HSCT were available for 38 of the 50 patients. Total IgG titers against VZV at these 3 points were monitored by ELISA. A 96-well microtiter plate (Nunc-Immuno Plate, MaxiSorp) was coated with 50 μL of VZV purified protein (AbD Serotec, Oxford, United Kingdom) diluted to 5 μg/mL overnight at 4°C. After blocking for 1 hour, 100 μL of patient plasma diluted 1:50 was added to the wells in duplicate. After incubation at room temperature for 2 hours, the plate was washed 3 times. Diluted peroxidase-conjugated rabbit antihuman IgG was added and incubated for 1 hour at room temperature. After 3 washes, an ABTS peroxidase substrate system was added to each well and the plate was read with a plate reader at 405 nm. Measles-specific IgG were analyzed in the same way using measles virus antigen (Meridian Life Science, Memphis, TN). The COI was calculated as described above.

To evaluate the magnitude of the serial changes in virus-specific IgG titer, a reduction rate for each patient was calculated by dividing the COI at 6 or 12 months after HSCT by the COI before HSCT.

Measurement of VZV-Specific and Measles-Specific IgG1m(f)

IgG1m(f) titer against VZV was also monitored sequentially for 12 allotype-informative patients. A 96-well microtiter plate was coated with 50 μL of VZV purified protein diluted to 5 μg/mL overnight at 4°C. After blocking for 1 hour, 100 μL of patient plasma diluted 1:5 was added to the wells in duplicate. After incubation at room temperature for 2 hours, the plate was washed 3 times. The mouse monoclonal antibody specific for G1m(f) was added at 1:2000 dilution and incubated for 2 hours at room temperature, and this was followed by 1 hour of incubation with peroxidase-conjugated antimouse IgG whole molecule antibody (A4416; Sigma, 1:2000 dilution). After 3 washes, the ABTS peroxidase substrate system was added to each well and the plate was read with a plate reader at 405 nm. Measles-specific IgG1m(f) were analyzed in the same way using measles virus antigen. The COI was calculated as described previously.

Statistical Analysis

The nonparametric Wilcoxon signed rank test and Fisher exact test were used to evaluate the statistical significance of differences in the IgG1m(f) value and in the incidence of the reduction or disappearance of virus-specific IgG. Statistical significance in a longitudinal data analysis of IgG or IgG1m(f) titer was assessed by the Jonckheere-Terpstra test. All statistical analyses were performed with EZR (Saitama Medical Center, Jichi Medical University, Saitama, Japan), which is a graphical user interface for R version 2.13.0 (R Foundation for Statistical Computing, Vienna, Austria) [14]. More precisely, it is a modified version of R commander (version 1.6-3) that was designed to add statistical functions that are frequently used in biostatistics.

Table 1
Patient Information

Characteristic	n
Sex (male/female)	28/22
Age, median (range), yr	46.5 (18-65)
Underlying disease	
AML	24
ALL	2
CML	1
MDS	2
NHL	4
ATL	6
MM	1
SAA	6
MF	1
Other	3
Stem cell source	
PB	19
BM	26
CB	5
Donor type	
Matched sibling	15
Mismatched relative	5
Unrelated	30
Conditioning regimen	
Conventional	26
RIC	24
IgG1m(f) allotype	
Donor (+) recipient (+)	3
Donor (−) recipient (+)	3
Donor(+) recipient (−)	9
Donor(−) recipient(−)	35

AML indicates acute myeloblastic leukemia; ALL, acute lymphoblastic leukemia; CML, chronic myeloid leukemia; MDS, myelodysplastic syndrome; NHL, non-Hodgkin lymphoma; ATL, adult T cell leukemia/lymphoma; MM, multiple myeloma; SAA, severe aplastic anemia; MF, myelofibrosis; PB, peripheral blood; BM, bone marrow; CB, cord blood; RIC, reduced-intensity conditioning.

RESULTS

IgG Allotype Information and History of VZV Disease

Fifty patient-donor pairs were analyzed with regard to the IgG allotype. The characteristics of the patients are shown in Table 1. Twelve pairs were informative because only the donor (n = 3) or the recipient (n = 9) was homozygous null for the IgG1m(f) allotype by ELISA assay and genotyping. Among these 12 informative patients, 4 developed VZV disease after discontinuing ACV administration. The others showed no clinical episode of VZV reactivation (Table 2). No patients experienced VZV disease during administration of low-dose ACV prophylaxis.

Appearance of Donor-Derived IgG and Disappearance of Recipient-Derived IgG after HSCT

Nine homozygous allotype–null patients with a IgG1m(f)-positive donor could be analyzed for the appearance of donor-derived IgG. One month after HSCT, donor-derived IgG1m(f) was detected in all but 1 patient. By 1 year after HSCT, donor-derived IgG1m(f) increased to almost the same levels as those in healthy donors. One patient who received RIC (Patient 8 in Table 2) remained negative for IgG1m(f) 6 months after HSCT (Figure 1A).

Among IgG1m(f)-positive patients with an allotype-null donor, the recipient-derived IgG1m(f) titer was gradually reduced, and it became negative by 6 months in 1 patient who received conventional conditioning (Patient 10 in Table 2). However, recipient-derived IgG1m(f) remained for more than 1 year after HSCT in the 2 patients who received RIC (Patients 11 and 12 in Table 2, Figure 1B).

Sequential Changes in VZV-Specific and Measles-Specific IgG

VZV-specific (n = 39) and measles-specific (n = 37) IgG titers after HSCT were analyzed concurrently among patients for whom sequential plasma samples were available. Two patients were measles IgG negative before HSCT. Both VZV and measles IgG titers gradually reduced during the following year ($P = .068$ and $P < .001$, respectively). Measles antibodies became negative (COI < 1) at 1 year after HSCT in 14 of 37 patients (37.8%), whereas only 5 of 39 patients (12.8%) became negative for VZV IgG ($P = .017$) (Figure 2A). In

Table 2
Profiles of the Twelve Informative Patients with or without VZV Disease

Patients with VZV Disease				
Characteristic	Patient 1	Patient 2	Patient 3	Patient 4
Age, yr	58	50	56	65
Sex	F	M	F	M
Disease	ATL	ALL	NHL	AML
Donor type	Unrelated BM	Related PB	Cord blood	Unrelated BM
Conditioning regimen	FLU+MEL	TBI+CY	FLU+MEL+TBI	FLU+MEL
Acute GVHD	–	–	–	–
Chronic GVHD	Oral, eye from d 450	–	–	–
IgG1m(f) (donor)	+	+	+	+
IgG1m(f) (recipient)	–	–	–	–
VZV disease	d 529	d -28 and d 410	d 720	d 665
Use of immunosuppressants at the onset	CsA	–	–	–
Skin region	Limited	Limited	Limited	Limited
Treatment	Oral VCV	Oral VCV	Oral VCV	Oral VCV
Postherpetic neuralgia	–	+	–	–
Outcome	CR	Relapse at d 230	CR	CR
Patients without VZV Disease				
Characteristic	Patient 5	Patient 6	Patient 7	Patient 8
Age, yr	40	42	31	58
Sex	M	F	F	M
Disease	CML-BC	SAA	AML	Other
Donor type	unrelated BM	unrelated BM	related PB	unrelated BM
Conditioning regimen	TBI+CY	TBI+CY	TBI+CY	FLU+TBI
Acute GVHD	Grade 2 from d 14	Grade 1 from d 35	Grade 1 from d 26	Grade 1from d 16
Chronic GVHD	Lung from d 201	Oral, eye from d 144	Liver from d 188	Muscle from d 125
IgG1m(f) (donor)	+	+	+	+
IgG1m(f) (recipient)	–	–	–	–
Characteristic	Patient 9	Patient 10	Patient 11	Patient 12
Age, yr	57	49	18	60
Sex	M	M	F	M
Disease	AML	AML	SAA	AML
Donor type	Related PB	Cord blood	Related PB	Unrelated BM
Conditioning regimen	FLU+ivBU	TBI+CY	FLU+CY+TBI	FLU+MEL
Acute GVHD	Grade 2 from d 35	–	–	–
Chronic GVHD	GI, liver from d 137	Oral, liver from d 219	GI from d 485	Liver from d 201
IgG1m(f) (donor)	+	–	–	–
IgG1m(f) (recipient)	–	+	+	+

VZV indicates varicella-zoster virus; M, male; F, female; ATL, adult T cell leukemia/lymphoma; ALL, acute lymphoblastic leukemia; NHL, non-Hodgkin lymphoma; AML, acute myeloblastic leukemia; BM, bone marrow; PB, peripheral blood; FLU, fludarabine; MEL, melphalan; CY, cyclophosphamide; TBI, total body irradiation; GVHD, graft-versus-host disease; d, day; CsA, cyclosporine; VCV, valacyclovir; CR, complete remission; CML, chronic myeloid leukemia; BC, blast crisis; SAA, severe aplastic anemia; ivBU, intravenous busulfan; GI, gastrointestinal.

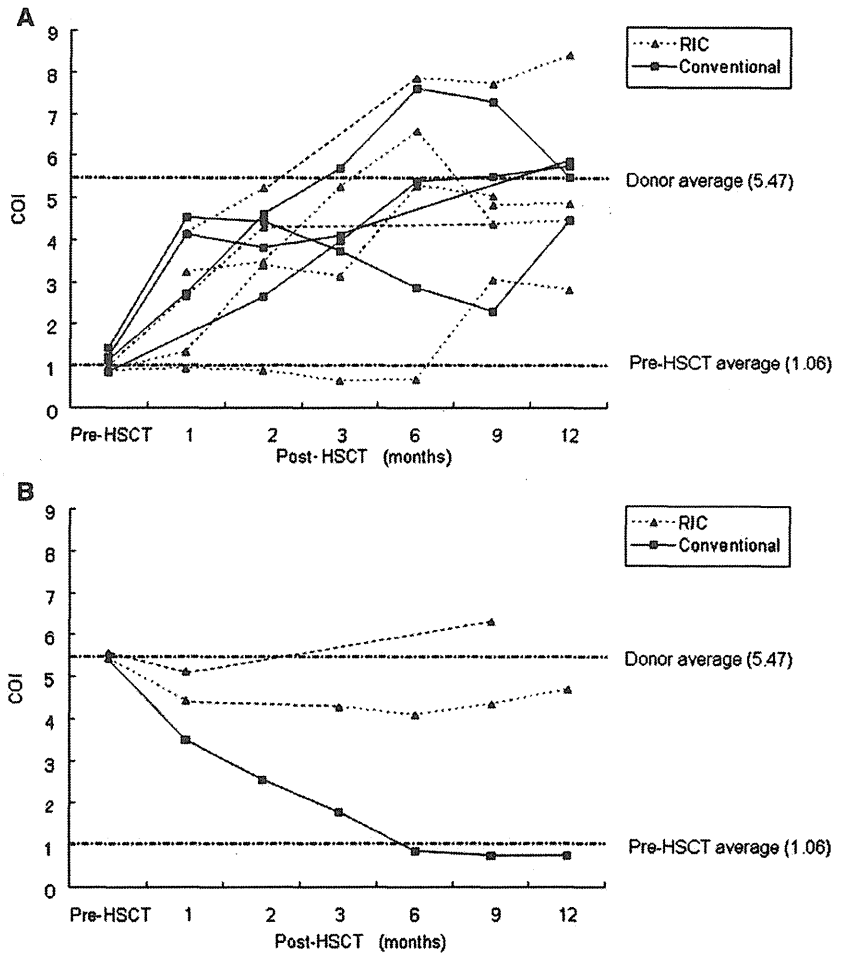

Figure 1. Serial changes in donor-derived (A) and recipient-derived (B) IgG1m(f) levels after allogeneic HSCT. Expression of the IgG1m(f) allotype was evaluated by an ELISA assay using anti-IgG1m(f) antibody. The Y-axis shows the cut-off index (COI) that was calculated as the mean OD^{405} from a sample divided by the cut-off value defined as the mean OD^{405} from negative controls plus 2-fold standard deviation.

addition, we compared the reduction rate from the IgG value before HSCT to those at 6 or 12 months after HSCT between VZV and measles (Figure 2B). Although both IgG titers were equivalently reduced by about 20% during the first 6 months ($P = .144$), the reduction rate of VZV IgG over 12 months was significantly lower than that of measles-IgG ($P = .004$).

Sequential Changes in VZV-Specific and Measles-Specific Donor-Derived IgG1m(f)

Eight of the 9 homozygous-null patients with IgG1m(f)-positive donors were analyzed sequentially (Figure 3). One patient (Patient 2 in Table 2) who showed an exceptionally high VZV IgG titer because of recent VZV infection was excluded. The COI for both the VZV-specific and measles-specific donor-derived IgG1m(f) remained low, at around 1.0, within 1 year after HSCT, and a significant trend for increased IgG1m(f) was not observed ($P = .237$ and $P = .131$, respectively). However, 3 patients became weakly positive (COI $\geq$ 1.5) for VZV IgG1m(f) at 6 to 9 months after HSCT. Thereafter, each of these 3 patients developed VZV disease after the discontinuation of ACV prophylaxis and the VZV IgG1m(f) titer was elevated to almost the same level as in healthy donors.

Sequential Changes in VZV-Specific and Measles-Specific Recipient-Derived IgG1m(f)

Three IgG1m(f)-positive patients with allotype-null donors were analyzed sequentially. Two patients who underwent HSCT using RIC regimens from IgG1m(f) null donors remained positive for recipient-derived IgG against VZV for over 1 year after HSCT, whereas in the remaining patient who received a conventional regimen (Patient 10 in Table 2), recipient-derived VZV IgG1m(f) titer became undetectable at 1 year after HSCT. A similar tendency was seen in a measles assay (data not shown).

Relationship Between the Clinical Course and the Change in Donor-Derived VZV-Specific IgG

Serial changes in donor-derived IgG1m(f) against VZV after HSCT in 4 patients who developed VZV reactivation are shown in Figure 4. All of the 4 patients were IgG1m(f) null patients with IgG1m(f)-positive donors. Patient 1 was a 58-year-old female with adult T cell leukemia who developed limited zoster on day 529. Although the donor-derived VZV IgG1m(f) titer had become weakly positive at around 30 days after HSCT, the IgG1m(f) titers against VZV were definitely elevated after the development of zoster. Patient 2 was a 50-year-old male with acute lymphoblastic leukemia whose

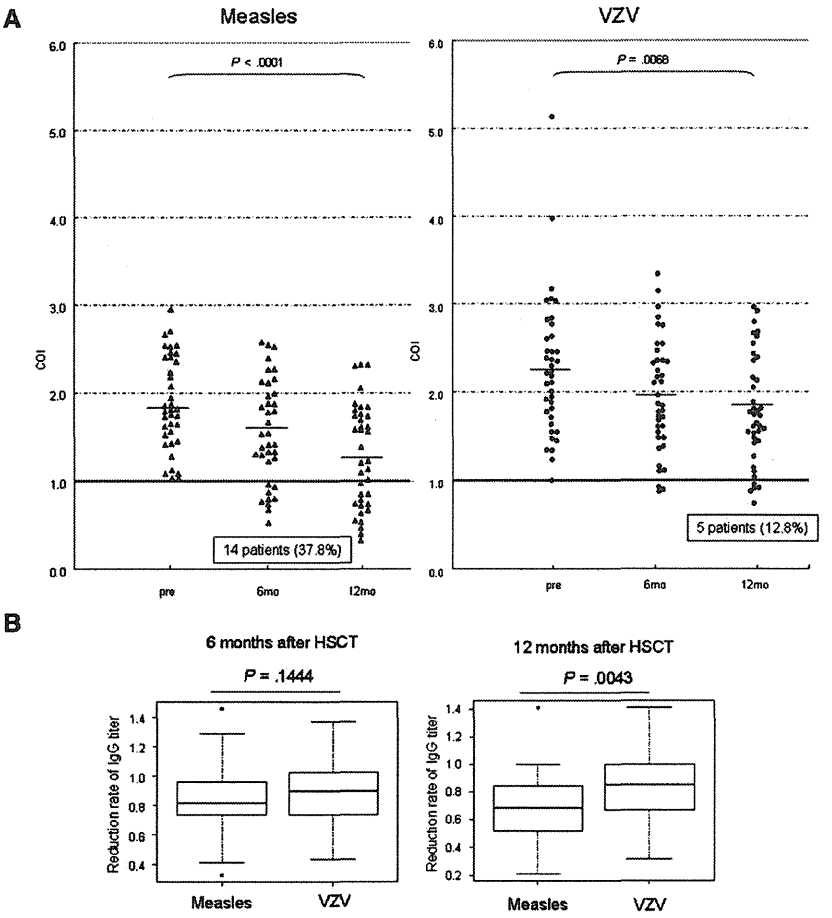

Figure 2. (A) Sequential changes in measles-specific (left) and varicella-zoster virus (VZV)-specific (right) IgG levels before and at 6 and 12 months after hematopoietic stem cell transplantation (HSCT). Triangles (measles) and circles (VZV) show individual data points. Mean values are shown by black lines. *P* values represent Jonckheere-Terpstra test. (B) The reduction rate at 6 (left) and 12 months (right) after HSCT. Box plots show the 25th and 75th percentiles and median values. *P* values represent nonparametric Wilcoxon signed rank test.

donor-derived anti-VZV IgG1m(f) was elevated at 6 months after HSCT. He suffered from localized zoster 1 month before HSCT, which was complicated by severe postherpetic neuralgia. Although he had a relapse of leukemia at day 230, VZV IgG1m(f) continued to increase until his second VZV disease at day 410. Patient 3 was a 56-year-old female with follicular lymphoma who underwent cord blood transplantation. In this case, although the cord blood donor was negative for VZV IgG, the VZV IgG1m(f) titers were slightly elevated at around 3 months after HSCT. These gradually reduced until the second elevation after VZV disease on day 720. Patient 4 was a 65-year-old female with acute myeloblastic leukemia who developed limited zoster on day 665. As in Patient 1, the donor-derived VZV IgG1m(f) titer became weakly positive at around 30 days after HSCT and remained weakly positive for more than 1 year. It was definitely elevated after the development of zoster.

DISCUSSION

Allotype-specific monoclonal antibodies can bind to single amino acid polymorphisms located in the immunoglobulin constant region of specific IgG isotypes. If either the donor or recipient is homozygous null for an allotype, the HSCT pair is informative with regard to the origin of antibody. This approach has been used to investigate donor-derived humoral immunity reconstitution after allogeneic HSCT [10]. In the current study, we focused on 1 of the IgG allotypes, IgG1m(f). Boiko et al. previously examined the expression of IgG1m(f) and IgG2m(n) in 63 HSCT donor-recipient pairs, 41% of which were informative [15]. Perhaps because of racial differences and the difficulty of obtaining anti-IgG2m(n) monoclonal antibody, only 12 of the 50 pairs in this study were informative. The allelic frequency of IgG1m(f) was 18 of 100 samples (18%), which is a slightly higher frequency than in previous Japanese reports [16,17].

Using such an allotype analysis, van Tol et al. showed the persistence of recipient-derived IgG at 3 to 8 years after myeloablative HSCT in a pediatric study [18]. More recently, Boiko et al. confirmed the persistence of recipient-derived humoral immunity after allogeneic HSCT using a RIC regimen by the detection of DNA chimerism in $CD38^{+}CD138^{+}$ plasma cells from bone marrow at 12 months after HSCT [15,19]. In the current study, 2 IgG1m(f)-positive patients who received a RIC regimen maintained recipient-derived VZV IgG for more than 1 year after HSCT. This was probably because of the persistence of recipient-derived plasma cells [20].

With regard to long-term immunity to various viruses, Ljungman et al. reported that the probabilities of being immune to measles at 3, 5, and 7 years after HSCT were 47%,

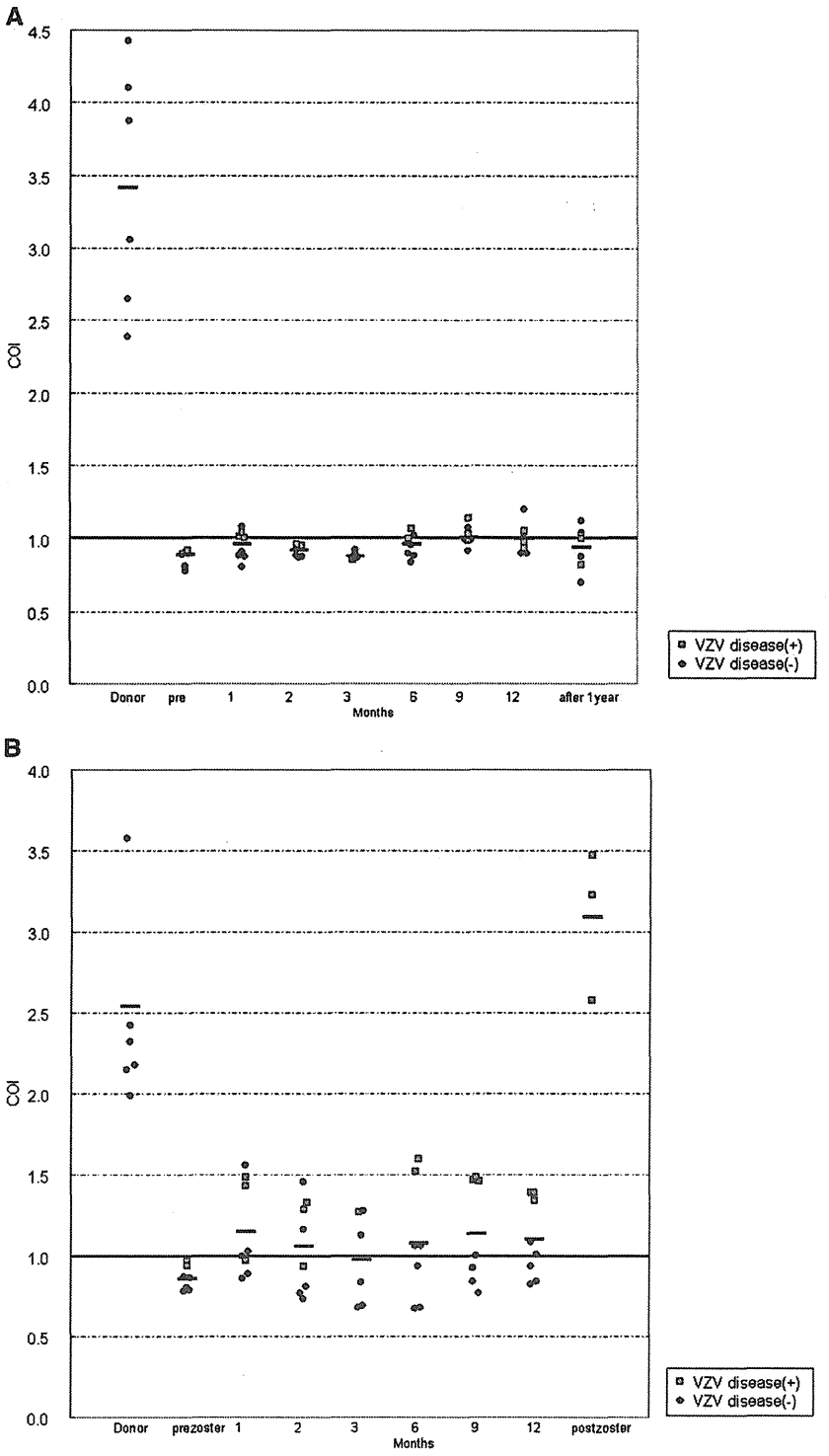

Figure 3. Sequential changes in measles-specific (A) and varicella-zoster virus (VZV)-specific (B) donor-derived IgG1m(f) levels. Gray and black squares indicate patients with and without VZV disease, respectively. Black lines show the mean values at the same points.

27%, and 20%, respectively. The corresponding probabilities were 37%, 12%, and 6% for mumps, and 47%, 33%, and 28% for rubella. They concluded that most allogeneic HSCT patients will become seronegative to nonlatent viruses during follow-up and long-term immunity, defined as persistent antibody not maintained regardless of the immune status of the donor [21]. However, since VZV is a latent and persistent virus, the time course of the disappearance of IgG after HSCT may be different from those of these nonlatent viruses. In our current analysis, the reduction rate of VZV IgG during